Canadian Science Publishing | Canadian Geotechnical Journal

Characterization of Model Uncertainty in Predicting Axial Resistance of Piles Driven into Clay

Journal:	*Canadian Geotechnical Journal*
Manuscript ID	cgj-2018-0386.R1
Manuscript Type:	Article
Date Submitted by the Author:	13-Sep-2018
Complete List of Authors:	Tang, Chong; National University of Singapore, Phoon, Kok-Kwang; National University of Singapore, Department of Civil & Environmental Engineering
Keyword:	Model uncertainty, Axial resistance, Driven piles, Clay, Load and resistance factor design
Is the invited manuscript for consideration in a Special Issue? :	Not applicable (regular submission)

Characterization of Model Uncertainty in Predicting Axial Resistance of Piles Driven into Clay

Chong Tang[1], Kok-Kwang Phoon[2]

[1]Research fellow, Department of Civil and Environmental Engineering, National University of Singapore, Block E1A, #07-03, 1Engineering Drive 2, Singapore 117576, E-mail: ceetc@nus.edu.sg

[2]Professor, Department of Civil and Environmental Engineering, National University of Singapore, Block E1A, #07-03, 1Engineering Drive 2, Singapore 117576, E-mail: kkphoon@nus.edu.sg

Abstract: This paper summarizes 239 static load tests to evaluate the performance of four static design methods for axial resistance of driven piles in clay. The methods are ISO 19901-4:2016, SHANSEP, ICP-05, and NGI-05. The database is categorized into four groups depending on the load type (compression or uplift) and pile tip condition (open or closed end). The model uncertainty in resistance prediction is quantified as a ratio between measured and calculated resistance, which is called a model factor. The measured resistance is interpreted as a load producing a settlement level of 10% pile diameter. Database studies show that four methods present a similar accuracy, where the mean and coefficient of variation (COV) of the model factor are around 1 and 0.3 respectively. The COV values are smaller than those for driven piles in sand available in literature. The model statistics determined from the database are also applicable to a simplified or full probabilistic form of reliability-based design (RBD) of driven piles in clay. As an illustration, the resistance factors in load and resistance factor design (LRFD, a simplified format of RBD) are calibrated by Monte Carlo simulations.

Keywords: Model uncertainty, Axial resistance, Driven piles, Clay, Load and resistance factor design

Introduction

Background

Numerous studies have been implemented to deliver a better understanding of the behaviour of driven piles in clay (Seed and Reese 1955; Peck 1958; Randolph et al. 1979; Blanchet et al. 1980; Morrison 1984; Jardine 1985; Azzouz and Lutz 1986; Chin 1986; Coop 1987; Bond 1989; Poulos 1989; Lehane 1992; Miller 1994; Chow 1997; McCabe 2002; Doherty 2010; Karlsrud 2012; Chen et al. 2014; Karlsrud et al. 2014; Haque et al. 2017). Factors that have an impact on driven pile behaviour were identified. Based on the experimental observations, various semi-empirical approaches were proposed to predict the axial pile resistance according to Eq. (1), which is calculated as the sum of the tip R_t and the shaft resistances R_s (Salgado 2008)

$$R_{uc} = R_s + R_t = \pi \cdot B \cdot \int \tau_f dz + r_t \cdot A_t \tag{1}$$

where R_{uc} is the calculated ultimate pile resistance, τ_f is the local ultimate shaft resistance, z is the depth to the ground surface, B is the pile diameter or width, r_t is the ultimate unit tip resistance over the pile tip area, and A_t is the pile tip area.

Eq. (1) assumes that the pile tip and shaft are moved sufficiently with respect to the adjacent soil to simultaneously develop the shaft and tip resistances. Although the displacement needed to mobilize the shaft resistance is generally smaller than that required to mobilize the tip resistance, this assumption was widely used for piles with diameter or width smaller than 914 mm (36 inches) (Hannigan et al. 2016). Open-end piles with diameter of 914 mm or greater are not considered in the present work. This pile type presents a unique challenge for practical engineers owing to the combination of several factors (Brown and Thompson 2015): (*i*) soil plug during pile installation is highly uncertain which has a significant effect on pile behavior; (*ii*) installation difficulty and potential damage during driving; (*iii*) difficulty in estimation of axial resistance from internal friction; and (*iv*) difficulty in verifying large nominal axial resistance with conventional load testing.

Review of design methods

To derive an analytically tractable model, physical and geometrical assumptions and simplifications are inevitably made. For instance, the unit tip resistance r_t is frequently taken from plasticity solutions (Hannigan et al. 2016)

$$r_t = N_c \cdot s_u \tag{2}$$

where N_c is the dimensionless bearing capacity factor, which is usually selected as 9 and s_u is the undrained shear strength.

Many studies were previously performed to predict the ultimate shaft resistance. The proposed methods can be grouped into four broad categories (Karlsrud 2014):

1. α-methods (Tomlinson 1957; Dennis and Olson 1983; Semple and Rigden 1984; Randolph and Murphy 1985; Kolk and van der Velde 1996; Karlsrud et al. 2005; Van Dijk and Kolk 2010; Karlsrud 2014), in which the ultimate shaft resistance is directly related to the undrained shear strength

$$\tau_f = \alpha \cdot s_u \tag{3}$$

where α is the adhesion factor which could be a function of s_u or s_u/σ_{v0}', in which σ_{v0}' is the effective vertical stress; pile length D; and/or other parameters.

2. β-methods (Burland 1973; Jardine et al. 2005; Karlsrud 2014), in which the ultimate shaft resistance is correlated to the effective vertical stress σ_{v0}'

$$\tau_f = \beta \cdot \sigma_{v0}' \tag{4}$$

where β is a coefficient equal to the ultimate shaft resistance normalized to the effective vertical stress, which could also depend on soil properties and pile geometries.

3. λ-method (Vijayvergiya and Focht 1972), a combination of α and β methods, which depends on the undrained shear strength and effective vertical stress

$$\tau_f = \lambda \cdot \left(a \cdot \sigma_{v0}' + b \cdot s_u\right) \tag{5}$$

where λ is a coefficient equal to the ultimate shaft resistance normalized to the combination of the undrained shear strength and effective stress, a and b are constants.

4. In situ test-based methods which directly relate the ultimate shaft resistance to the in situ test results, such as standard penetration test (SPT) (Meyerhof 1976) or cone penetration test (CPT) (Lehane et al. 2013). They eliminate the intermediate estimation of soil engineering parameters.

Detailed summaries of the methods for resistance calculation can be found in Doherty and Gavin (2011) and Niazi (2014). It is clearly observed some empirical coefficients (e.g. α, β, and λ) are involved within these methods, which were usually calibrated against pile load test (typically limited). The deviation of the predicted from the measured resistance would be expected, because of the simplifications, assumptions, and approximations made in the respective design model. This deviation is expressed as model uncertainty (Lacasse and Nadim 1996; Lacasse et al. 2013a, b; Phoon et al. 2016; Lesny 2017), which is of epistemic nature (Nadim 2015).

Objective of this study

The fourth edition of ISO 2394 (General Principles on Reliability for Structures) (International Organization for Standardization 2015) now contains a new informative Annex D on "Reliability of Geotechnical Structures". ISO 2394:2015 is meant to be used as a basis for national/international code committees to draft design codes where the principles of risk and reliability are utilized (Phoon 2016). The model uncertainty was identified as one of critical elements of geotechnical reliability-based design (RBD) process in Annex D (Phoon et al. 2016).

Accordingly, the primary objective of this paper is to characterize the model uncertainty in calculating the axial resistance of driven piles in clay by (*i*) α-methods in ISO 19901-4:2016 (ISO 2016) and Karlsrud et al. (2005), (*ii*) β-method in Jardine et al. (2005), and (*iii*) the stress history and normalized soil engineering parameter (SHANSEP) concept in Saye et al. (2013). To this end, an integrated database of 239 field static load tests which are compiled from literature is developed. The quantified model uncertainty are then applied to calibrate the resistance factors in load and resistance factor design (LRFD) of driven piles in clay using Monte Carlo simulations with the load statistics in AASHTO LRFD specification (AASHTO 2014).

Representation of model uncertainty

Following the Annex D of ISO 2394:2015, the model uncertainty is simply represented as the ratio of the measured resistance to the calculated resistance:

$$M_{\mathrm{u}} = \frac{R_{\mathrm{um}}}{R_{\mathrm{uc}}} \tag{6}$$

where M_{u} is the resistance model factor and R_{um} is the measured resistance. This approach is practical, but realistically grounded on the load test database. On the other hand, Lesny (2017) commented that the model factor approach could reach its limits where obvious deficiencies exist in the design model such as offshore pile foundation under combined loading (e.g. vertical structural load and lateral wave force).

Evaluation of the resistance model factor consists of the computation of mean and coefficient of variation (COV) and identification of probability distribution. A model factor with an excessively large COV may indicate that the respective design model does not capture the key features of the problem. Resistance model statistics and application in LRFD of of driven piles can be found in Paikowsky et al. (2004), Su (2005), Abu-Farsakh et al. (2009), Yang and Liang (2006, 2009), Kwak et al. (2010), Dithinde et al. (2011), AbdelSalam et al. (2012), Vu (2013), Machairas et al. (2018), and Tang and Phoon (2018a-c). For each type of pile tip (open or closed end) under compression or uplift, dataset used in the previous studies remain surprisingly small (Lacasse and Nadim 1996; Paikowsky et al. 2004; Lacasse et al. 2013a, b; Lehane et al. 2013; Saye et al. 2013; Karlsrud 2014).

It should be noted that the main problem of using database to characterize the model uncertainty is the limited number of tests from different sources with each covering only a limited range of possible design situations (Lesny 2017).

Estimation Methods for Pile Shaft Resistance

ISO 19901-4:2016

The absolute value of the undrained shear strength was adopted early to evaluate the adhesion factor α such as the method of Tomlinson (1957). In contrast, Semple and Ridgen (1994) first introduced the normalized strength as a basis for the α-value. Subsequently, this concept was widely employed. In Chapter 8 "Pile foundation design" of ISO 19901-4:2016 (ISO 2016), the adhesion factor α varies based on effective stress and is computed as

$$\begin{aligned} \alpha &= 0.5 \cdot \Psi^{-0.5} \qquad \Psi \le 1 \\ \alpha &= 0.5 \cdot \Psi^{-0.25} \qquad \Psi > 1 \end{aligned} \tag{7}$$

with $\alpha \le 1$, where $\Psi = s_u/\sigma_{v0}'$. Kolk and van der Velde (1996) proposed a similar format to Eq. (7), but includes a length factor. Unconsolidated-undrained (UU) triaxial compression tests on high quality sample are recommended for establishing the undrained shear strength because of their consistency and repeatability.

NGI-05 method

Over the past 30 years, the Norwegian Geotechnical Institute (NGI) carried out a number of field load tests on driven piles. It was recognized that the plasticity index could have a large influence on the shaft resistance. In this context, a new calculation method, called NGI-05, was presented in Karlsrud et al. (2005), where the α-value is given below

$$\alpha = 0.32\left(I_{\mathrm{p}} - 10\right)^{0.3} \tag{8}$$

for normally consolidated (NC) clay with $0.2<\alpha<1$ and $\Psi<0.25$ and

$$\alpha = 0.5 \cdot \Psi^{-0.3} \cdot F_{\mathrm{t}} \tag{9}$$

for overconsolidated (OC) clay with $\Psi>1$, where I_{p} is the plasticity index and F_{t} is the correction factor=1 for open-end pile and $0.8+0.2\cdot\Psi^{0.5}$ for closed-end pile. For clay with $0.25<\Psi<1$, α is estimated by an interpolation between $\Psi=0.25$ and 1 from a semi-log plot in Karlsrud et al. (2005). The reference strength within the NGI-05 method is the UU triaxial strength.

Karlsrud (2012) argued that the undrained shear strength from direct simple shear (DSS) test is a more appropriate representation of the strength characteristics, as this mode of shearing is most comparable to that of a soil element along the axially loaded pile shaft (Karlsrud 2014). A modified version of the NGI-05 method was developed in Karlsrud (2014), where the DSS undrained shear strength was utilized to determine the α-coefficient for different values of the plasticity index.

SHANSEP-based approach

Saye et al. (2013) presented a method to estimate the shaft resistance of driven pipe pile in clay using the SHANSEP concept. In this approach, the shaft resistance τ_{f} is treated as an adhesion, which is normalized with respect to σ_{v0}'. The normalized adhesion is then related to the soil overconsolidation ratio (OCR) in the same format as the concept for normalized undrained shear strength given by Ladd and Foott (1974), which is given below

$$\frac{\tau_{\mathrm{f}}}{\sigma'_{\mathrm{v0}}} = \left(\frac{\tau_{\mathrm{f}}}{\sigma'_{\mathrm{v0}}}\right)_{\mathrm{NC}} \cdot \mathrm{OCR}^{m} \tag{10}$$

which separates the NC from the OC behavior, where τ_f/σ_{v0}' is the normalized side adhesion, $[\tau_f/\sigma_{v0}']_{NC}$ is the normalized side adhesion of NC clay=0.19, m=0.7 for an exponent representing the increasing in with OCR, and OCR is evaluated as

$$\mathrm{OCR} = \left(\frac{\Psi}{0.32}\right)^{1.25} \quad (11)$$

where the undrained shear strength is determined from UU triaxial compression test or unconfined compression (UC) test.

As discussed in Saye et al. (2013), the SHANSEP-based approach provides the means to address many of the limitations of conventional empirical correlations of axial resistance with undrained shear strength. Saye et al. (2016) examined the effect of sample disturbance on laboratory undrained shear strength tests used in the SHANSEP-based approach to predict the ultimate shaft resistance of driven closed-end pipe piles. For cohesive soils with OCR<2, sample disturbance was identified as a significant factor affecting the ultimate shaft resistance. With removing the case histories from the database in Saye et al. (2013) that were likely affected by sample disturbance, an equivalent α-method was produced by Saye et al. (2016), where $\alpha=0.51\cdot\Psi^{-0.12}$.

It has been stated above that the UU undrained shear strength is preferable in the methods of ISO 19901-4:2016, NGI-05, and SHANSEP. Another type of shear strength such as consolidated-isotropically undrained triaxial compression (CIUC) and UC test can be converted into the UU type using the relations in Chen and Kulhawy (1993).

ICP-05 method

The β-methods in Eq. (4) are effective stress analyses based on the theory of lateral earth pressure, expressed as

$$\tau_f = K_\delta \cdot \tan\delta_f \cdot \sigma'_{v0} \quad (12)$$

where K_δ is the coefficient of lateral earth pressure, δ_f is the friction angle of the soil-pile interface, and the coefficient β is a product of K_δ and $\tan\delta_f$. Burland (1973) suggested a typical range of β=0.25-0.4 for soft clays and K_δ was assumed to be the coefficient of lateral earth pressure at rest for stiff clays, but without a clear recommendation for tanδ_f. A double-log design chart for the β-coefficient was presented in Karlsrud (2014) for different values of plasticity index and OCR.

Randolph (2003) mentioned that a scientific approach to determine the shaft resistance of a driven pile should consider the complex stress-strain history. The mechanisms governing the pile behaviour can be categorized into the following phases (Doherty and Gavin 2011): (*i*) prior to installation, stresses within soil correspond to in situ state; (*ii*) stresses within soil increase during pile installation; (*iii*) stresses will change due to the dissipation of pore-water pressure, residual loads and age-related effects, resulting in an equalized radial stress prior to loading; and (*iv*) applied load may induce additional increases in radial stress on the shaft due to interface dilation, eventually reaching failure at peak radial stresses.

Based on the enhanced understanding of pile behaviour, Jardine et al. (2005) proposed a new effective stress analysis method, called ICP-05, where ICP is an abbreviation of Imperial College Pile. The ICP-05 method made an attempt to account for the actual radial effective stress acting on the pile shaft surface and the K_δ and δ_f values are separately evaluated in a rational way:

$$\begin{aligned} &\tau_f = \sigma'_{rf} \cdot \tan\delta_f,\ \sigma'_{rf} = 0.8 \cdot \sigma'_{rc},\ \sigma'_{rc} = K_c \cdot \sigma'_{v0} \\ &K_c = \left(2.2 + 0.016 \cdot \mathrm{OCR} - 0.87 \cdot \log_{10} S_t\right) \cdot \mathrm{OCR}^{0.42} \cdot F_L \end{aligned} \tag{13}$$

where σ_{rf}' is the radial effective stress against the pile shaft at failure, σ_{rc}' is the radial effective stress against the pile shaft after full consolidation, K_c is the coefficient of radial effective earth pressure after full setup, S_t is the sensitivity which is defined as the ratio of intact and remoulded undrained shear strength, and F_L=[max(z/R^*, 8)]$^{-0.2}$, R^*=R_o=outer radius for closed-end pile and R=$(R_o^2$-$R_i^2)^{0.5}$ for open-end pile, R_i is the inner radius. The effects of pile length, diameter and tip condition (open- or closed-end) are considered in Eq. (13) with the geometric term F_L.

The basic assumption of Eq. (13) is that the ultimate shaft resistance is primarily controlled by the interface friction angle of reconstituted clay as determined by ring shear tests and the radial effective stress. If the measurement of OCR and S_t are unavailable, they can be determined from the known shear strength s_u and effective vertical stress σ_{v0}' via the relations in Augustesen (2006). For the friction angle δ_f

along the pile shaft-soil interface, there is no universal and reliable link to the plasticity index I_p, which it could be estimated from the best fit δ_f-I_p line in Jardine et al. (2005).

Database of Pile Load Tests

A database with well-documented field and laboratory test data plays a key role in piling industry, first and foremost in deriving more accurate and reliable design methods (Kolk and van der Velde 1996; Jardine et al. 2005; Karlsrud et al. 2005; Van Dijk and Kolk 2010; Lehane et al. 2013; Karlsrud 2014) and second in the calibration of current design methods or the characterization of model uncertainty in pile design which has been discussed earlier in this paper. Studies on the development of pile load test database were conducted by Olson and Dennis (1982), Briaud and Tucker (1988), Eslami and Fellenius (1997), Augustesen (2006), Roling et al. (2011), Niazi (2014), AbdelSalam et al. (2015), Abu-Hejleh et al. (2015), Yang et al. (2015), Lehane et al. (2017), Adhikari et al. (2018), Moshfeghi and Eslami (2018), and Tang and Phoon (2018a).

Lambe (1973) discussed that the quality of geotechnical prediction does not necessarily increase with the level of sophistication in the model. He opined that reasonable calculations can be obtained using simple models as long as there are sufficient data to calibrate these models empirically. Such an observation emphasizes the importance of data in geotechnical engineering. The full value of a database is arguably best realized within a direct probability-based design method (Wang et al. 2016). Recent development in the gradual adoption of RBD is more sensitive to information. The latest edition of the *Canadian highway bridge design code* (Canadian Standards Association 2014) introduces the concept of a resistance factor that depends on the “degree of understanding” (low, typical, high). Fenton et al. (2016) noticed that “there is a real desire amongst the geotechnical community to have their designs reflect the degree of their site and model understanding”. Site understanding is associated with how well the ground providing the geotechnical resistance is known and model understanding refers to the degree of confidence that a designer has in the model used to predict the geotechnical resistance.

For the purpose of this work, a global database is developed in Tables A1-A2 in Appendix A1. The measured resistances, pile geometries, and key soil engineering parameters are reported. The load test data are compiled from

1. Saldivar and Jardine (2005) reported 27 compression tests on concrete piles in Mexico City clay. Pre-boring was used in 26 static load tests to ease pile-driving difficulties. Little research was conducted on the possible effects of pre-boring, which are often ignored. All 27 tests are given in Table A1.
2. Augustesen (2006) collated a filtered database with 268 static load tests on concrete, steel and timber piles, which were collected from literature, Norwegian and Danish companies. The criteria to choose the data can be found in Augustesen (2006). 189 load tests on concrete and steel piles are adopted in Tables A1-A2.
3. Lehane et al. (2013) summarized 53 tests in Chow (1997) and 22 tests in literature, with complete CPT profile. Because 62 load tests have been considered by Augustesen (2006), the other 15 tests are integrated into Tables A1-A2.
4. Karlsrud (2014) presented 60 instrumented and 12 non-instrumented pile tests from previous studies. As 64 tests have been contained within the filtered database of Augustesen (2006), the other 8 uplift tests on steel open-end piles are included within Table A2.

The ranges of pile diameter, slenderness ratio and the normalized soil engineering parameters are given in Table 1. The load test regions cover Belgium, Canada, China, Denmark, Germany, Indonesia, Iran, Ireland, Italy, Mexico, Norway, Singapore, Sweden, Turkey, Thailand, United Kingdom, and United States. The clay parameters cover a wide range of plasticity index I_p (10-160), sensitivity S_t (1-17), and overconsolidation ratio OCR (1-43). The pile diameter or width ranges between 0.1 and 0.81. The collected 239 static load tests on driven piles in clay is divided into four groups: (*i*) 115 compression tests on closed-end pile (65 for concrete and 55 for steel), (*ii*) 60 compression tests on open-end steel pipe pile, (*iii*) 32 uplift tests on closed-end pile (7 for concrete and 25 for steel), and (*iv*) 32 uplift tests on open-end steel pipe pile.

It is very common in practice that many pile load tests are not carried out to failure, where the corresponding load-settlement curves do not show a clear peak. Therefore, the measured resistance in Eq. (6) usually refers to an interpreted value from the measured load-settlement data with a certain criterion. Marcos et al. (2013) evaluated the bias in resistance interpretation criteria for driven precast concrete piles in compression for drained and undrained condition. Studies associated with the effect of bias in failure criteria on the model statistics and reliability analysis were performed by Phoon and Kulhawy (2005) and Zhang et al. (2005). In this article, the measured resistance is defined as the load corresponding to a pile head settlement of 10% of the pile diameter *B*. It is very easy to apply in practice and allows both the tip and shaft resistances to be fully mobilized as possible.

Probabilistic Evaluation of Resistance Model Factor

Uncertainty in resistance calculation

For driven pile in clay, the calculated resistances using the ISO 19901-4:2016, NGI-05 (Karlsrud et al. 2005), ICP-05 (Jardine et al. 2005), and SHANSEP-based methods (Saye et al. 2013) are summarized in Tables A1-A2 in Appendix A1. They are plotted against the measured resistances in Fig. 1. It can be seen that the mean trend lines are quite close to the equality line. Fig. 2 shows that the resistance model factor M_u takes a range of values. Uncertainty in resistance prediction could be attributed to the following factors:

1. Theoretical imperfections of the α-methods (Doherty and Gavin 2011) are that (*i*) soil behavior governed by effective stress and the change in the stress-strain relation arising from the pile installation cannot be completely described by the initial undrained strength profile and (*ii*) the effect of the friction along the soil-shaft interface on the location of failure surface on which the shear resistance develops is not considered.
2. Idealization of the soil profile as homogeneous clay for each site when clay exists along more than 70% of the profile (AbdelSalam et al. 2012). In reality, spatial variability is an intrinsic feature of a site profile.

3. Measurement errors in pile load test and test to determine soil engineering parameters (e.g. s_u, OCR, and S_t) and transformation errors within the models used to estimate soil properties and the interface friction angle δ_f, when accurate measurement is unavailable. Selection of soil parameters is subjective and different pile resistances can be obtained even for the same design model (Karlsrud 2014).
4. Empiricisms involved within these methods, in which the α- and β-coefficients or lateral earth pressure coefficient K_c were calibrated against few load test data. When the design scenario (e.g. pile geometries and/or soil properties) is outside the domain of the calibration database, additional uncertainty will be introduced.
5. Uncertainty associated with the procedure and measurement technique used in load tests. Tomlinson (1995) stated that the rate of load application in a load test is different than that of a building under construction.
6. Bias in the definition and interpretation of the measured resistance from a load test.

In short, the model factor in Eq. (6) is a lumped variable covering many sources of uncertainties (i.e. spatial variability, measurement and transformation errors, and bias in the interpretation of load test data) (Lesny 2017).

Verification of randomness

As discussed in Phoon et al. (2016), the model factors may not be random in the sense that it is systematically affected by input parameters such as problem geometry. In this situation, it may not be appropriate to treat the model factor as a random variable directly. Examples can be found in Zhang et al. (2015), Tang and Phoon (2017) and Tang et al. (2017a, b). Therefore, the randomness should be verified, prior to compute the mean and COV values and identify the probability distribution.

The observed values for the resistance model factor M_u are plotted against pile diameter B in Fig. 3, slenderness ratio D/B in Fig. 4, normalized shear strength Ψ=s_u/σ_{v0}' in Fig. 5, overconsolidation ratio OCR in Fig. 6, plasticity index I_p in Fig. 7, and sensitivity S_t in Fig. 8. Except for M_u of ISO 19901-4:2016 and

NGI-05 with respect to D/B, visual inspection suggests no major dependence exists between M_u and the input parameters.

The randomness is further verified with the presence or absence of correlation between the model factors and input parameters. The correlation is assessed using the Matlab function "corr". The returning results are the r-value (i.e. correlation) and the p-value (i.e. probability). If the p-value is less than 0.05, the correlation r is significantly different from zero. The results from the Spearman rank correlation analyses are summarized in Table A3 in Appendix A2. Some p-values are lower than 0.05, suggesting the model factor may depend on the underlying parameter. For example of driven open-end pile in axial compression, the model factor for ISO 19901-4:2016 appears to decrease as slenderness ratio D/B increases, as shown in Fig. 4a. This implies that the α-coefficient could be affected by D/B. Several previous studies attempted to express the α-coefficient as a function of D/B to consider the potential length effect (Dennis and Olson 1983; Semple and Rigden 1984; Kolk and van der Velde 1996). Nevertheless, the most associated r-values vary between 0 and 0.4, indicating no or negligible to a moderate degree of correlation. For simplicity, the model factors of four design methods are still assumed to be random variables.

Discussion and comparison of model statistics

The model statistics are given in Table 2. For driven piles in clay, the ranges of mean and COV are 1.05-1.08 and 0.31-0.34 (closed-end piles in compression), 0.92-1.11 and 0.26-0.29 (closed-end piles in uplift), 0.97-1.16 and 0.24-0.3 (open-end piles in compression), 0.85-1.01 and 0.27-0.39 (open-end piles in uplift). For each pile type, differences in the statistics of the resistance model factor M_u for four methods are not very significant. The results imply that these methods present a consistent accuracy. Similar observation was reported in Lehane et al. (2013, 2017). For steel pipe piles, the mean and COV of the NGI-05 method for the UU shear strength are 1.05 and 0.26. They are close the values of 1.04 and 0.2 for the revised NGI-05 method with the DSS shear strength (Karlsrud 2014). Augustesen (2006) also found that the model statistics with s_u conversion were comparable to those without s_u conversion. The results suggest that these methods might be statistically insensitive to errors in interpreted s_u.

According to Saye et al. (2016), the sample disturbance for clay with OCR<2 is considerably influential to measure s_u or preconsolidation stress σ_p' and therefore affects the calculation of shaft resistance. It is interesting to compare the performance of four design models for clay with OCR<2 and OCR>2. In this regard, the observed resistance model factors for OCR<2 and OCR>2 are plotted against the measured resistances in Fig. 2, which does not differentiate the pile type (closed or open end) and load direction (compression or uplift). The difference within the observed model factors is not discernible. This can be further verified with the statistics. For OCR<2 (74 cases), the mean and COV values of M_u are 0.93 and 0.38 for ISO 19901-4:2016, 0.96 and 0.25 for NGI-05, 1.09 and 0.31 for SHANSEP, and 1.09 and 0.3 for ICP-05. The results are comparable to those for OCR>2 (164 cases), with 1.03 and 0.31 for ISO 19901-4:2016, 1.06 and 0.29 for NGI-05, 1.08 and 0.29 for SHANSEP, and 1.02 and 0.32 for ICP-05. On this basis, there is no need to derive the model statistics respectively for OCR<2 and OCR>2.

For comparison purposes, the model statistics available in literature are also given in Table 2. Different model statistics are obtained even for the same design method, which is closely related to the calibration database. The model uncertainty in predicting axial resistance of driven piles in sand is generally higher than that of driven piles in clay, because of the extreme levels of soil distortion during pile installation (Randolph 2003).

Identification of probability distribution

The probability distribution functions of the observed model factors are determined from the Kolmogorov-Smirnov goodness-of-fit test. It measures the compatibility of a sample with a theoretical probability distribution function. The observed values for the resistance model factor M_u for driven piles under axial compression are presented in Fig. 9 which follows a lognormal distribution. The model factors for driven piles under axial uplift are given in Fig. 10, which may follow a lognormal or weibull distribution. It is noteworthy that the number of uplift load tests for each type of pile tip is much smaller than that of compression load tests.

Application of Model Statistics in LRFD calibration

Limit state equation

The Federal Highway Administration (FHWA) mandated the use of LRFD for all new bridges initiated after September 2007. LRFD may be the most popular simplified RBD format in North America. In the United States, the nationwide survey of AbdelSalam et al. (2012) indicated that the resistance factors were mainly derived by fitting to the factor of safety based on the experience. Recently, more state Department of Transportation in the United States calibrated the region-specific resistance factors by reliability theory such as California (Caltrans 2014), Indiana (Salgado et al. 2011), Iowa (AbdelSalam et al. 2012), Louisiana (Abu-Farsakh et al. 2009), Illinois (Long and Anderson 2014), Missouri (Luna 2014), Minnesota (Paikowsky et al. 2014), Texas (Seo et al. 2015), and Wyoming (Adhikari et al. 2018).

The limit state equation in foundation design can be defined in terms of resistance and applied load. The foundation will fail if the resistance is less than the applied load and otherwise, the foundation performs satisfactorily. These situations can be concisely described as follows

$$g\left(R,Q\right)=R-Q \tag{14}$$

where R is the resistance and Q is the applied load. The basic objective of RBD is that the probability of failure does not exceed an acceptable level:

$$p_{\mathrm{f}}=\Pr\left(R-Q\le 0\right)\le p_{\mathrm{fT}} \tag{15}$$

where p_{f} is probability of failure, Pr is the symbol for probability, and p_{fT} is target probability of failure. The reliability index β_{r} is estimated from $\mathrm{p_f}$ as follows

$$\beta_{\mathrm{r}}=-\Phi^{-1}\left(p_{\mathrm{f}}\right) \tag{16}$$

where Φ^{-1}= inverse standard normal cumulative function.

The basic design equation for LRFD is given by (AASHTO 2014)

$$\psi_{\mathrm{R}}R_{\mathrm{n}}\ge\sum\gamma_{\mathrm{i}}Q_{\mathrm{ni}} \tag{17}$$

where R_{n} is the calculated nominal resistance, ψ_{R} is the resistance factor applicable to R_{n}, Q_{ni} is the specific nominal load, and γ_{i} is the load factor applicable to Q_{ni}. By considering the AASHTO Strength Limit I (i.e. the combination of dead load Q_{DL} and live load Q_{LL}), the applied load is then written as

$$Q = \lambda_{\mathrm{DL}} Q_{\mathrm{DL}} + \lambda_{\mathrm{LL}} Q_{\mathrm{LL}} \tag{18}$$

where λ_{DL} is the bias of Q_{DL} and λ_{LL} is the bias of Q_{LL}. In AASHTO (2014), the load bias factors λ_{DL} and λ_{LL} are assumed to be lognormally distributed. The mean and COV of λ_{DL} are 1.05 and 0.1, while the mean and COV of λ_{LL} are 1.15 and 0.2.

Calibration of resistance factor

Setup refers to the increase in axial resistance of driven piles after end of driving, which has been studied by many researchers (Bullock et al. 2005; Augustesen 2006; Ng et al. 2013a; Chen et al. 2014; Karlsrud et al. 2014; Haque et al. 2017; Haque and Abu-Farsakh 2018). It is attributed to three main mechanisms: (*i*) dissipation of excess pore water pressure (consolidation effect), (*ii*) regaining of soil strength with time (thixotropic effect), and (*iii*) increasing soil strength with time (aging effect). The widely used setup estimation model expresses the ratio of resistances at time t after pile driving and at time t_0 of end of driving as a logarithmic function of t/t_0 (Skov and Denver 1988; Karlsrud et al. 2005; Ng et al. 2013b; Haque and Abu-Farsakh 2018). Incorporating setup into design might result in cost saving by means of reducing the number of piles, shortening the pile length, reducing the pile cross-sectional area, or reducing the size of pile driving equipment (Haque and Abu-Farsakh 2018). Integration of setup in LRFD can be found in Yang and Liang (2006, 2009), Ng and Sritharan (2016), and Haque and Abu-Farsakh (2018).

Because the time of pile driving and test for most case histories in Appendix A1 is not reported, setup is not considered in this work. The performance function in Eq. (14) is further expressed as the following simple format (Abu-Farsakh et al. 2009)

$$g = \left(\frac{\gamma_{\mathrm{DL}} + \gamma_{\mathrm{LL}} / \eta}{\psi_{\mathrm{R}}} \right) M_{\mathrm{u}} - \left(\lambda_{\mathrm{DL}} + \lambda_{\mathrm{LL}} / \eta \right) \tag{19}$$

where γ_{DL} is the dead load factor=1.25, γ_{LL} is the live load factor=1.75, and η is the ratio of dead to live load=$Q_{\mathrm{DL}}/Q_{\mathrm{LL}}$. Three steps are implemented to calibrate the resistance factor ψ_{R} (Abu-Farsakh et al. 2009):

1. Select a trial resistance factor and generate random numbers for three random variables (i.e. M_u, λ_{DL}, and λ_{LL}) in Eq. (19);
2. Find the number N_f of cases where the performance function in Eq. (19) is not greater than zero and p_f=N_f/N_s (N_s=total number of Monte Carlo simulations=1,000,000 here).
3. Repeat step Nos. 1 and 2 until $|\beta_r$-$\beta_T|$<tolerance=0.01, where β_T=the target reliability index=2.33 for redundant piles and 3 for non-redundant piles (Paikowsky et al. 2004).

The above reliability calibration is similar to that proposed by Phoon et al. (2003). As an illustration, variation of ψ_R with load ratio η=Q_{DL}/Q_{LL}=1~10 for ICP-05 method is shown in Fig. 11 for β_T=2.33 and 3. It presents ψ_R decreases nonlinear with an increasing η. After $\eta\geq3$, ψ_R almost becomes constant for all cases. This has also been observed by Paikowsky et al. (2004), AbdelSalam et al. (2012), Abu-Farsakh et al. (2009) and Tang and Phoon (2018a-c). The resistance factors for η=3 with β_T=2.33 and 3 are summarized in Table 3. It is observed that β_T has a more pronounced influence than η on ψ_R. For example of closed-end piles under compression, ψ_R reduces from 0.53 to 0.41 (23% reduction) for ISO 19901-4:2016 when β_T increases from 2.33 up to 3. In addition, Paikowsky et al. (2004) mentioned that the efficiency factor ψ_R/μ, where μ is the mean model factor, represents the effectiveness of the respective design model. The efficiency factors are also given in Table 3.

Summary and Conclusions

This paper collated an integrated database with 115 and 60 compression tests on closed and open-end piles and 32 and 32 uplift tests on closed and open-end piles. The database was utilized to characterize the model uncertainty in calculating the axial resistance of driven piles in clay by the α-methods (ISO 19901-4:2016 and NGI-05), β-method (ICP-05), and the SHANSEP-based approach. Statistical analyses were implemented to determine the mean, COV and probability distribution of the model factor. From a statistical viewpoint, four methods presented similar performance where the mean and COV of the model factor are equal to 1 and 0.3 approximately. The COV values are found to be smaller than those driven piles in sand.

The model statistics were then utilized to calibrate the resistance factors in LRFD of driven piles in clay. It should be noted that the model statistics are also applicable to a full probabilistic form of RBD. One needs to keep in mind that the application of the derived model statistics beyond the database boundaries should be verified (ideally by more high-quality load test results) (Lesny 2017). Low (2017) and Phoon (2017) explained in detail that RBD can play a complementary role to LRFD within the prevailing norms of geotechnical practice. For instance, RBD is very useful to deal with complex real-world information (multivariate correlated soil data) and information imperfections (scarcity of information or incomplete information). It is also very useful to handle spatial variability of a site profile that cannot be easily treated in deterministic means.

References

AASHTO. 2014. AASHTO LRFD Bridge Design Specifications. 7th ed. American Association of State Highway and Transportation Officials, Washington, D.C.

AbdelSalam, S.S., Sritharan, S., Suleiman, M.T., Ng, K.W., and Roling, M.J. 2012. Development of LRFD Design Procedures for Bridge Pile Foundations in Iowa. Vol. III: Recommended Resistant Factors with Consideration to Construction Control and Setup. Report No. IHRB Projects TR-584, Iowa Department of Transportation, February, 2012.

AbdelSalam, S.S., Baligh, F.A., and El-Naggar, H.M. 2015. A database to ensure reliability of bored pile design in Egypt. Proceedings of the Institution of Civil Engineers-Geotechnical Engineering, 168(2): 131-143. doi:10.1680/geng.14.00051.

Abu-Farsakh, M.Y., Yoon, S.M., and Tsai, C. 2009. Calibration of resistance factors needed in the LRFD design of driven piles. Report No. FHWA/LA.09.449, Louisiana Transportation Research Center, May 2009.

Abu-Hejleh, N.M., Abu-Farsakh, M., Suleiman, M.T., and Tsai, C. 2015. Development and use of high-quality databases of deep foundation load tests. Transportation Research Record: Journal of the Transportation Research Board, No. 2511: 27-36. doi:10.3141/2511-04.

Adhikari, P., Gebreslasie, Y.Z., Ng, K.W., Sullivan, T.A., and Wulff, S.S. 2018. Static and dynamic analysis of driven piles in soft rocks considering LRFD using a recently developed electronic database. *In* IFCEE 2018: Installation, Testing, and Analysis of Deep Foundations (GSP 294), *edited by* M.T. Suleiman, A. Lemnitzer, and A.W. Stuedlein, 83-92. Reston, VA: ASCE.

Augustesen, A.H. 2006. The effects of time on soil behaviour and pile capacity. Ph.D. thesis, Aalborg University.

Azzouz, A.S., and Lutz, D.G. 1986. Shaft behavior of a model pile in plastic empire clays. Journal of Geotechnical Engineering, 112(4): 389-406. doi:10.1061/(ASCE)0733-9410(1986)112:4(389).

Blanchet, R., Tavenas, F., and Garneau, R. 1980. Behavior of friction piles in soft sensitive clays. Canadian Geotechnical Journal, 17(2): 203-224. doi:10.1139/t80-023.

Bond, A.J. 1989. Behaviour of displacement piles in overconsolidated clays. Ph.D. thesis, Imperial College London.

Briaud, J.L., and Tucker, L.M. 1988. Measured and predicted axial response of 98 piles. J. Geotech. Engrg. 114 (9): 984-1001. doi:10.1061/(ASCE)0733-9410(1988)114:9(984).

Brown, D.A., and Thompson III, W.R. 2015. Design and load testing of large diameter open-ended driven piles. Report NCHRP Synthesis 478. Transportation Research Board, Washington, D.C.

Bullock, P.J., Schmertmann, J.H., McVay, M.C., and Townsend, F.C. 2005. Side shear setup. II: Results from Florida test piles. Journal of Geotechnical and Geoenvironmental Engineering, 131(3): 301-310. doi:10.1061/(ASCE)1090-0241(2005)131:3(301).

Burland, J.B. 1973. Shaft friction of piles in clay: A simple fundamental approach. Ground Engineering, 6(3): 1-15.

Caltrans. 2014. Calibrating LRFD geotechnical axial (tension and compression) resistance factors (ψ) for driven piles and drilled shafts. Research notes, Caltrans Division of Research, Innovation and System Information.

Canadian Standards Association. 2014. Canadian Highway Bridge Design Code. CAN/CSA-S6-14, Mississauga, Ontario.

Chen, Y.J., and Kulhawy, F.H. 1993. Undrained strength interrelationships among CIUC, UU, and UC tests. Journal of Geotechnical Engineering, 119(11): 1732-1750. doi:10.1061/(ASCE)0733-9410(1993)119:11(1732).

Chen, Q., Haque, M.N., Abu-Farsakh, and Fernandez, B.A. 2014. Field investigation of pile setup in mixed soil. Geotechnical Testing Journal, 37(2): 268-281. doi:10.1520/GTJ20120222.

Chin, C.T. 1986. Open-ended pile penetration in saturated clays. Ph.D. thesis, Massachusetts Institute of Technology.

Chow, F. 1997. Investigation into the behavior of displacement piles for offshore structures. Ph.D. thesis, Imperial College London.

Coop, M.R. 1987. The axial capacity of driven piles in clay. Ph.D. thesis, Oxford University.

Dennis, N.D., and Olson, R.E. 1983. Axial capacity of steel pipe piles in clay. *In* Proceedings of the Conference on Geotechnical Practice in Offshore Engineering, Austin, Texas. *Edited by* S.G. Wright, 370-388.

Dithinde, M., Phoon, K.-K., Wet, M.D., and Retief, J.V. 2011. Characterization of model uncertainty in the static pile design formula. Journal of Geotechnical and Geoenvironmental Engineering, 137(1): 70-85. doi:10.1061/(ASCE)GT.1943-5606.0000401.

Doherty, P. 2010. Factors affecting the capacity of open and closed-ended piles in clay. Ph.D. thesis, University College Dublin.

Doherty, P., and Gavin, K. 2011. The shaft capacity of displacement piles in clay: a state of the art view. Geotechnical and Geological Engineering, 29(4): 389-410. doi:10.1007/s10706-010-9389-2.

Eslami A., and Fellenius, B.H. 1997. Pile capacity by direct CPT and CPTu methods applied to 102 case histories. Canadian Geotechnical Journal, 34(6): 886-904. doi:10.1139/cgj-34-6-886.

Fenton, G.A., Naghibi, F., Dundas, D., Bathurst, R.J., and Griffiths, D.V. 2016. Reliability-based geotechnical design in 2014 Canadian Highway Bridge Design Code. Canadian Geotechnical Journal, 53(2): 236-251. doi:10.1139/cgj-2015-0158.

Hannigan, P.J., Rausche, F., Likins, G.E., Robinson, B.R., and Becker, M.L. 2016. Design and Construction of Driven Pile Foundations. Vol. I. Publication No. FHWA-NHI-16-009, U.S. Department of Transportation, Federal Highway Administration, September 2016.

Haque, M.N., Abu-Farsakh, M.Y., Tsai, C., and Zhang, Z.J. 2017. Load-testing program to evaluate pile-setup behavior for individual soil layers and correlation of setup with soil properties. Journal of Geotechnical and Geoenvironmental Engineering, 143(4): 04016109. doi:10.1061/(ASCE)GT.1943-5606.0001617.

Haque, M.N., and Abu-Farsakh, M.Y. 2018. Estimation of pile setup and incorporation of resistance factor in load resistance factor design framework. Journal of Geotechnical and Geoenvironmental Engineering, 144(11): 04018077. doi:10.1061/(ASCE)GT.1943-5606.0001959.

International Organization for Standardization. 2015. General principles on reliability of structures. ISO2394:2015, Geneva, Switzerland.

International Organization for Standardization. 2016. Petroleum and natural gas industries-specific requirements for offshore structures. Part 4: geotechnical and foundation design considerations. ISO 19901-4:2016, Geneva, Switzerland.

Jardine, R.J. 1985. Investigation of pile soil behaviour with special reference to the foundations of offshore structures. Ph.D. thesis, Imperial College London.

Jardine, R.J., Chow, F., Overy, R., and Standing, J. 2005. ICP design methods for driven piles in sand and clays. Thomas Telford, London.

Karlsrud, K., Clausen, C., and Aas, P. 2005. Bearing capacity of driven piles in clay, the NGI approach. *In* Proceedings of 1st International Symposium on Frontiers in Offshore Geotechnics (ISFOG 2005), Perth, Australia. *Edited by* S. Gourvenec and M. Cassidy. CRC Press/Balkema, 775-782.

Karlsrud, K. 2012. Prediction of load-displacement behavior and capacity of axially loaded piles in clay based on interpretation of load test results. Ph.D. thesis, Norwegian Univ. of Science and Technology, Trondheim, Norway.

Karlsrud, K. 2014. Ultimate shaft friction and load-displacement response of axially loaded piles in clay based on instrumented pile tests. Journal of Geotechnical and Geoenvironmental Engineering, 140(12): 04014074. doi:10.1061/(ASCE)GT.1943-5606.0001170.

Karlsrud, K., Jensen, T.G., Lied, E.K.W., Nowacki, F., and Simonsen, A.S. 2014. Significant ageing effects for axially loaded piles in sand and clay verified by new field load tests. OTC-25197-MS. Offshore Technology Conference, Houston, Texas, USA.

Kolk, H.J., and van der Velde, E. 1996. A reliable method to determine the friction capacity of piles driven into clays. OTC-7993-MS. Offshore Technology Conference, Houston, Texas, USA.

Kwak, K., Kim, K.J., Huh, J.W., Lee, J.H., and Park, J.H. 2010. Reliability-based calibration of resistance factors for static bearing capacity of driven steel pipe piles. Canadian Geotechnical Journal, 47(5): 528-538. doi:10.1139/T09-119.

Lacasse, S., and Nadim, F. 1996. Model uncertainty in pile axial capacity calculations. OTC-7996-MS. Offshore Technology Conference, Houston, Texas, USA.

Lacasse, S., Nadim, F., Andersen, K.H., Eidsvig, U.K., Yetginer, G., Guttormsen, T.R., and Eide, A. 2013a. Reliability of API, NGI, ICP and Fugro axial pile capacity calculation methods. OTC-24063-MS. Offshore Technology Conference, Houston, Texas, USA.

Lacasse, S., Nadim, F., Langford, T., Knudsen, S., Yetginer, G.L., Guttormsen, T.R., and Eide, A. 2013b. Model uncertainty in axial pile capacity design methods. OTC-24066-MS. Offshore Technology Conference, Houston, Texas, USA.

Ladd, C.C., and Foott, R. 1974. New design procedure for stability of soft clays. Journal of the Geotechnical Engineering Division, 100(7): 763-786.

Lambe, T.W. 1973. Predictions in soil engineering. Géotechnique, 23(2): 151-202. doi:10.1680/geot.1973.23.2.151.

Lehane, B.M. 1992. Experimental Investigations of pile behaviour using instrumented field piles. Ph.D. thesis, Imperial College London.

Lehane, B.M., Li, Y.N., and Williams, R. 2013. Shaft capacity of displacement piles in clay using the cone penetration test. Journal of Geotechnical and Geoenvironmental Engineering, 139(2): 253-266. doi:10.1061/(ASCE)GT.1943-5606.0000749.

Lehane, B.M., Kim, J.K., Carotenuto, P., Nadim, F., Lacasse, S., Jardine, R.J., van Dijk, B.F.J. 2017. Characteristics of unified databases for driven piles. *In* Proceedings of 8th International Conference on Offshore Site Investigations and Geotechnics (OSIG 2017), London, UK. *Edited by* M.D.J. Sayer, G. Griffiths, and L.J. Ayling. Society for Underwater Technology, vol. 1, 162-191. doi:10.3723/OSIG17.162.

Lesny, K. 2017. Evaluation and consideration of model uncertainties in reliability based design. Chapter 2. *In* Final report for Joint ISSMGE TC 205/TC 304 Working Group on "Discussion of statistical/reliability methods for Eurocodes", September 2017.

Long, J., and Anderson, A. 2014. Improved design for driven piles based on a pile load test program in Illinois: phase 2. Report No. FHWA-ICT-14-019, Illinois Department of Transportation.

Low, B.K. 2017. Insights from reliability-based design to complement load and resistance factor design approach. Journal of Geotechnical and Geoenvironmental Engineering, 143(11): 04017089. doi:10.1061/(ASCE)GT.1943-5606.0001795.

Luna, R. 2014. Evaluation of Pile Load Tests for Use in Missouri LRFD Guidelines. Report No. cmr14-015, Missouri Department of Transportation.

Machairas, N., Highley, G.A., and Iskander, M.G. 2018. Evaluation of FHWA pile design method against the FHWA deep foundation load test database version 2. Transportation Research Record: Journal of the Transportation Research Board, in press. doi:10.1177/0361198118773196.

Marcos, M.C.M., Chen, Y.J., and Kulhawy, F.H. 2013. Evaluation of compression load test interpretation criteria for driven precast concrete pile capacity. KSCE Journal of Civil Engineering: Geotechnical Engineering, 13(5): 108-1022. doi:10.1007/s12205-013-0262-8.

McCabe, B. 2002. Experimental Investigations of driven pile group behaviour in Belfast soft clay. Ph.D. thesis, Trinity College Dublin.

Meyerhof, G.G. 1976. Bearing capacity and settlement of pile foundations. Journal of the Geotechnical Engineering Division, 102(3): 195-228.

Miller, G.A. 1994. Behavior of displacement piles in overconsolidated clay. Ph.D. thesis, University of Massachusetts Amherst, USA.

Morrison, M.J. 1984. In situ measurements on a model pile in clay. Ph.D. thesis, Massachusetts Institute of Technology.

Moshfeghi, S., and Eslami, A. 2018. Study on pile ultimate capacity criteria and CPT-based direct methods. International Journal of Geotechnical Engineering, 12(1): 28-39. doi:10.1080/19386362.2016.1244150.

Nadim, F. 2015. Accounting for uncertainty and variability in geotechnical characterization of offshore sites. *In* 5th International Symposium on Geotechnical Safety and Risk (ISGSR 2015). *Edited by* T. Schweckendiek, A.F. Van Tol, D. Pereboom, M. Van Staveren, and P.M. Cools, IOS press, 23-35. doi:10.3233/978-1-61499-580-7-23.

Ng, K.W., Roling, M., AbdelSalam, S.S., Suleiman, M.T., and Sritharan, S. 2013a. Pile setup in cohesive soil. I: experimental investigation. Journal of Geotechnical and Geoenvironmental Engineering, 139(2): 199-209. doi:10.1061/(ASCE)GT.1943-5606.0000751.

Ng, K.W., Suleiman, T.M., and Sritharan, S. 2013b. Pile setup in cohesive soil. II: Analytical quantifications and design recommendations. Journal of Geotechnical and Geoenvironmental Engineering, 139(2): 210–222. doi:10.1061/(ASCE)GT.1943-5606.0000753.

Ng, K.W., and Sritharan, S. 2016. A procedure for incorporating setup into load and resistance factor design of driven piles. Acta Geotechnica, 11(2): 347-358. doi:10.1007/s11440-014-0354-8.

Niazi, F.S. 2014. Static axial pile foundation response using seismic piezocone data. Ph.D. thesis, Georgia Institute of Technology.

Olson, R.E., and Dennis, N.D. 1982. Review and Compilation of Pile Test Results, Axial Capacity. Report GR83-4. Geotechnical Engineering Center, The University of Texas at Austin.

Paikowsky, S.G., Birgisson, B., McVay, M., Nguyen, T., Kuo, C., Baecher, G.B., Ayyub, B., Stenersen, K., O'Malley, K., Chernauskas, L., and O'Neill, M. 2004. Load and Resistance Factors Design for Deep Foundations. NCHRP Report 507, Transportation Research Board of the National Academies, Washington, D.C.

Paikowsky, S.G., Canniff, M., Robertson, S., and Budge, S.A. 2014. Load and Resistance Factor Design (LRFD) Pile Driving Project – Phase II Study. MnDOT Report No. MN/RC 2014-16, Minnesota Department of Transportation Research Services and Library.

Peck, R.B. 1958. A study of the comparative behaviour of friction piles. Highway Research Board, Special Report No. 36.

Phoon, K.-K., Kulhawy, F.H., and Grigoriu, M.D. 2003. Development of a reliability-based design framework for transmission line structure foundations. Journal of Geotechnical and Geoenvironmental Engineering, 129(9): 798-806. doi:10.1061/(ASCE)1090-0241(2003)129:9(798).

Phoon, K.-K., and Kulhawy, F.H. 2005. Characterisation of model uncertainties for laterally loaded rigid drilled shafts. Géotechnique, 55(1): 45-54. doi:10.1680/geot.2005.55.1.45.

Phoon, K.-K., Retief, J.V., Ching, J.Y., Dithinde, M., Schweckendiek, T., Wang, Y., and Zhang, L.M. 2016. Some observations on ISO 2394:2015 Annex D (Reliability of Geotechnical Structures). Structural Safety, 62: 24-33. doi:10.1016/j.strusafe.2016.05.003.

Phoon, K.-K. 2016. "Reliability of geotechnical structures." Proc., 15^{th} Asian Regional Conference on Soil Mechanics and Geotechnical Engineering, Japanese Geotechnical Society Special Publication, 1-9.

Phoon, K.-K. 2017. Role of reliability calculations in geotechnical design. Georisk: Assessment and Management of Risk for Engineered Systems and Geohazards, 11(1): 4-21. doi:10.1080/17499518.2016.1265653.

Poulos, H.G. 1989. Pile behaviour: theory and application. Géotechnique, 39(3): 365-415. doi:10.1680/geot.1989.39.3.365.

Randolph, M.F., Carter, J.P., and Wroth, C.P. 1979. Driven piles in clay-the effects of installation and subsequent consolidation. Géotechnique, 29(4): 361-393. doi:10.1680/geot.1979.29.4.361.

Randolph, M.F., and Murphy, B.S. 1985. Shaft capacity of driven piles in clay. OTC-4883-MS. Offshore Technology Conference, Houston, Texas, USA.

Randolph, M.F. 2003. Science and empiricism in pile foundation design. Géotechnique, 53(10): 847-875. doi:10.1680/geot.53.10.847.37518.

Roling, M.J., Sritharan, S., and Suleiman, M.T. 2011. Development of LRFD procedures for bridge pile foundations in Iowa. Volume I: An electronic database for pile load tests in Iowa (PILOT). Report No. IHRB Project TR-573, Iowa Department of Transportation.

Saldivar, E.E., and Jardine, R.J. 2005. Application of an effective stress design method to concrete piles driven in Mexico City clay. Canadian Geotechnical Journal, 42(6): 1495-1508. doi:10.1139/t05-062.

Salgado, R. 2008. The engineering of foundations. McGraw-Hill, New York

Salgado, R., Woo, S.I., and Kim, D. 2011. Development of load and resistance factor design for ultimate and serviceability limit states of transportation structure foundations. Report No. FHWA/IN/JTRP-2011/03, Indiana Department of Transportation.

Saye, S.R., Brown, D.A., and Lutenegger, A.J. 2013. Assessing adhesion of driven pipe piles in clay using adaptation of stress history and normalized soil engineering parameter concept. Journal of Geotechnical and Geoenvironmental Engineering, 139(7): 1062-1074. doi:10.1061/(ASCE)GT.1943-5606.0000842.

Saye, S.R., Lutenegger, A.J., Brown, D.A., and Kumm, B.P. 2016. Influence of sample disturbance on estimated side resistance of driven piles in cohesive soils. Journal of Geotechnical and Geoenvironmental Engineering, 142(10): 04016043. doi:10.1061/(ASCE)GT.1943-5606.0001517.

Seed, H.B., and Reese, L.C. 1955. The action of soft clay along friction piles. Transactions of the American Society of Civil Engineer, 122(1): 731-754.

Seo, H., Moghaddam, R.B., Surles, J.G., and Lawson, W.D. 2015. Implementation of LRFD geotechnical design for deep foundations using Texas cone penetrometer (TCP) test. Report No. FHWA/TX-16/6-6788-01-1, Texas Department of Transportation.

Semple, R.M., and Rigden, W.J. 1984. Shaft capacity of driven pipe piles in clay. *In* Proceedings of the Symposium on Analysis and Design of Deep Foundations, San Francisco. *Edited by* J.R. Meyer, 59-79.

Skov, R., and Denver, H. 1988. Time dependence of bearing capacity of piles. *In* Proceedings of 3rd International Conference on the Application of Stress-Wave Theory to Piles. *Edited by* B.H. Fellenius, Ottawa, Canada, 879-888.

Su, Y.T. 2005. Calibration of resistance factors for load and resistance factor design of driven piles for bridge foundations. Ph.D. thesis, Clemson University.

Tang, C., and Phoon, K.-K. 2017. Model uncertainty of Eurocode 7 approach for bearing capacity of circular footings on dense sand. International Journal of Geomechanics, 17(3): 04016069. doi:10.1061/(ASCE)GM.1943-5622.0000737.

Tang, C., Phoon, K.-K.. and Akbas, S.O. 2017a. Model uncertainties for the static design of square foundations on sand under axial compression. *In* Geo-Risk 2017: Reliability-based design and code developments (Geotechnical Special Publication 283), *Edited by* J.S. Huang, G.A. Fenton, L.M. Zhang, and D.V. Griffiths, 141-150.

Tang, C., Phoon, K.-K, Zhang, L., and Li, D.Q. 2017b. Model uncertainty for predicting the bearing capacity of sand overlying clay. International Journal of Geomechanics, 17(7): 04017015. doi:10.1061/(ASCE)GM.1943-5622.0000898.

Tang, C., and Phoon, K.-K. 2018a. Statistics of model factors and consideration in reliability-based design of axially loaded helical piles. Journal of Geotechnical and Geoenvironmental Engineering, 144(8): 04018050. doi:10.1061/(ASCE)GT.1943-5606.0001894.

Tang, C., and Phoon, K.-K. 2018b. Evaluation of model uncertainties in reliability-based design of steel H-piles in axial compression. Canadian Geotechnical Journal, doi:10.1139/cgj-2017-0170.

Tang, C., and Phoon, K.-K. 2018c. Statistics of model factors in reliability-based design of axially loaded driven piles in sand. Canadian Geotechnical Journal, doi:10.1139/cgj-2017-0542.

Tomlinson, M.J. 1957. The adhesion of piles driven in clay soils. *In* Proceedings of 4th International Conference on Soil Mechanics and Foundation Engineering, Vol. 2, Butterworths, London, 66-71.

Tomlinson, M.J. 1995. Pile design and construction practice. 4th ed. E & FN Spon, an imprint of Chapman & Hall, London, UK.

Van Dijk, B.F.J., and Kolk, H.J. 2010. CPT-based design method for axial capacity of offshore piles in clays. *In* Proceedings of 2nd International Symposium on Frontiers in Offshore Geotechnics (ISFOG 2010), Perth, Australia. *Edited by* S. Gourvenec and M. Cassidy. CRC Press/Balkema, 555-560.

Vijayvergiya, V.N., and Focht, J.A. 1972. A new way to predict capacity of piles in clay. OTC-1718-MS. Offshore Technology Conference, Houston, Texas, USA.

Vu, C. 2013. Geological dependence of resistance factors for deep foundation design. Ph.D. thesis, University of Colorado at Denver.

Wang, Y., Schweckendiek, T., Gong, W.P., Zhao, T.Y., and Phoon, K.-K. 2016. Direct probability-based design methods. Chapter 7. *In* Reliability of geotechnical structures in ISO 2394. *Edited by* K.-K. Phoon and J.V. Retief, 193-226. Boca Raton, FL: CRC Press.

Yang, L., and Liang, R. 2006. Incorporating setup into reliability-based design of driven piles in clay. Canadian Geotechnical Journal, 43(9): 946-955. doi:10.1139/t06-054.

Yang, L., and Liang, R. 2009. Incorporating setup into load and resistance factor design of driven piles in sand. Canadian Geotechnical Journal, 46(3): 296-305. doi:10.1139/T08-118.

Yang, Z.X., Jardine, R.J., Guo, W.B., and Chow, F. 2015. A comprehensive database of tests on axially loaded piles driven in sands. Zhejiang University Press and Elsevier.

Zhang, L.M., Li, D.Q., and Tang, W.H. 2005. Reliability of bored pile foundations considering bias in failure criteria. Canadian Geotechnical Journal, 42(4): 1086-1093. doi:10.1139/t05-044.

Zhang, D.M., Phoon, K.-K., Huang, H.W., and Hu, Q.F. 2015. Characterization of model uncertainty for cantilever deflections in undrained clay. Journal of Geotechnical and Geoenvironmental Engineering, 141(1): 04014088. doi:10.1061/(ASCE)GT.1943-5606.0001205.

List of Figure Caption

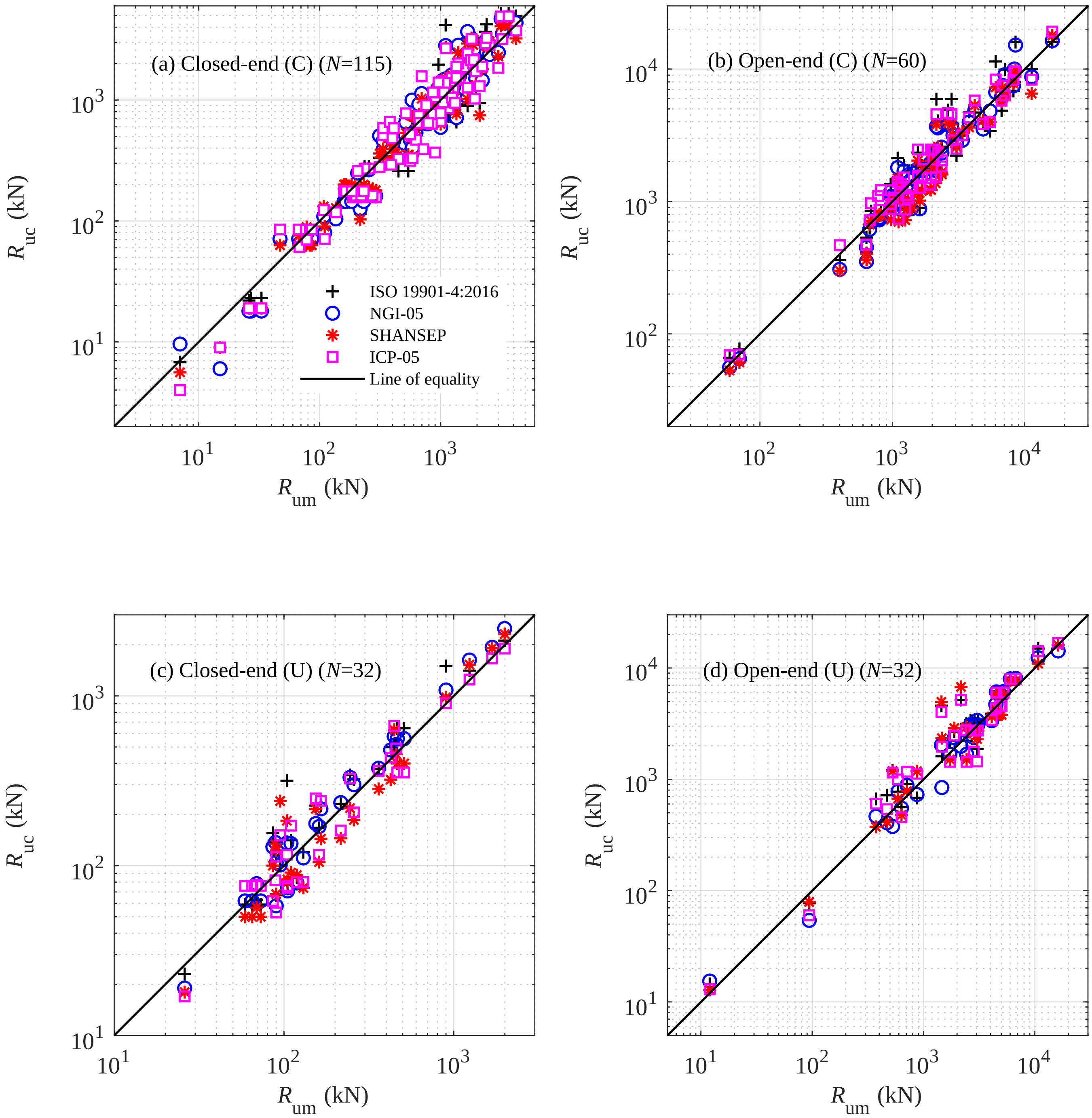

Fig. 1. Comparison of measured and calculated resistances for driven piles in clay

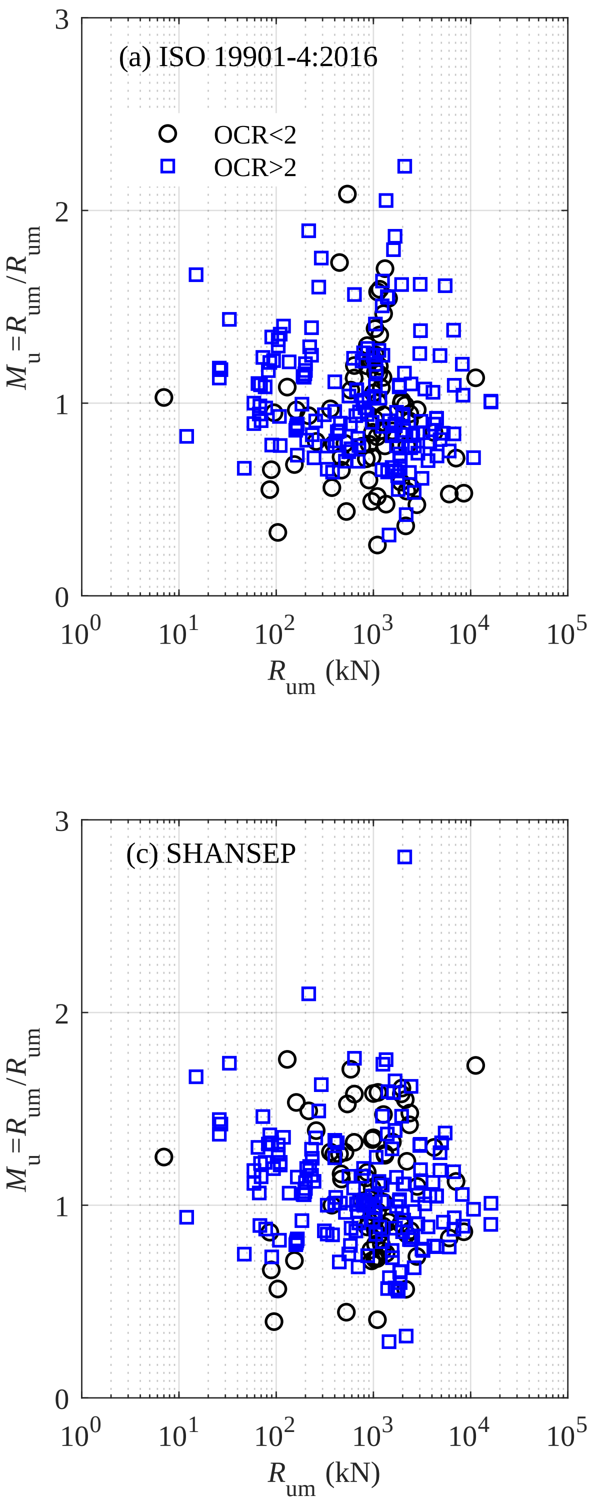

Fig. 2. Scatter plots of resistance model factor versus measured resistance for OCR<2 and OCR>2

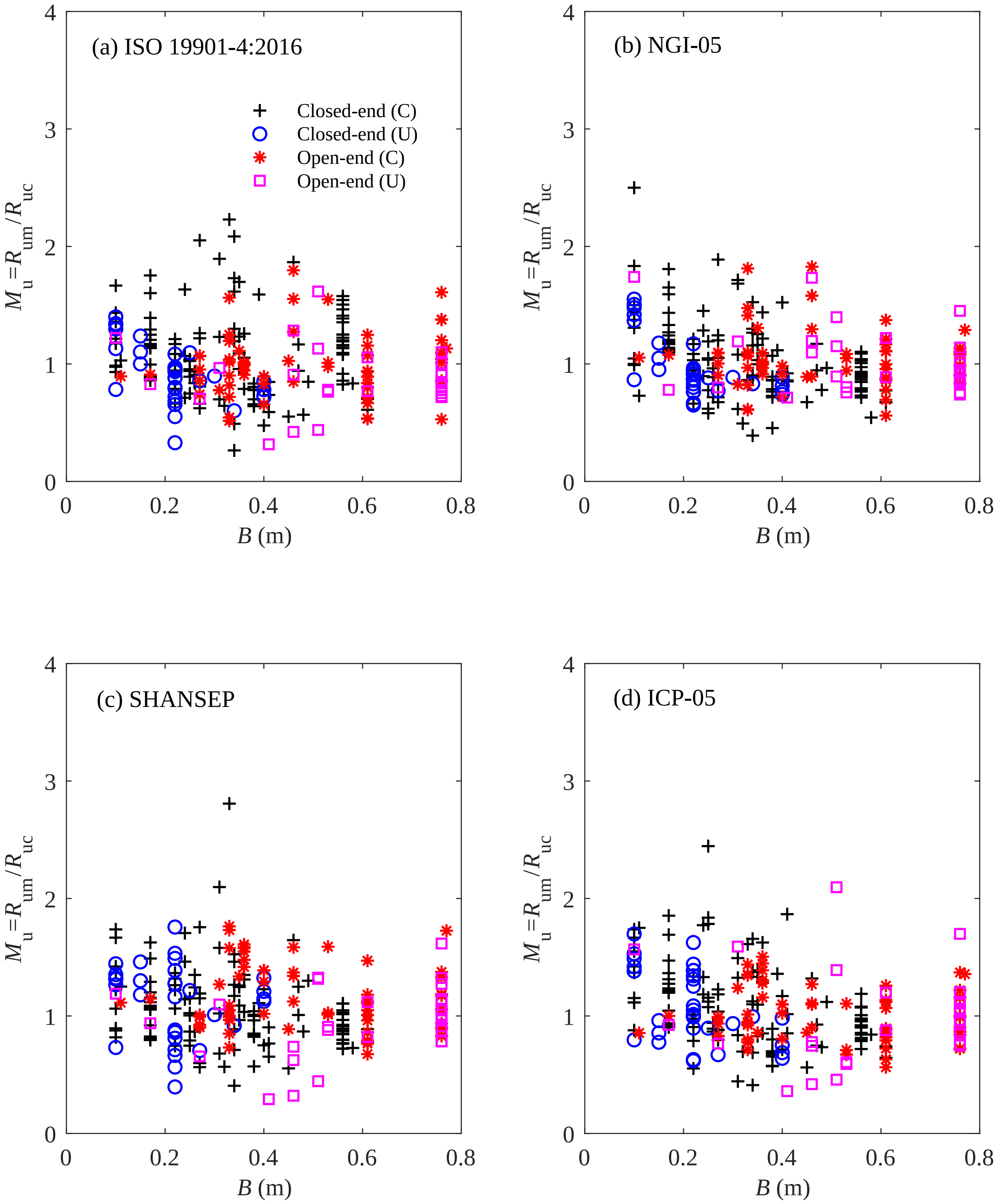

Fig. 3. Distributions of resistance model factor against pile diameter

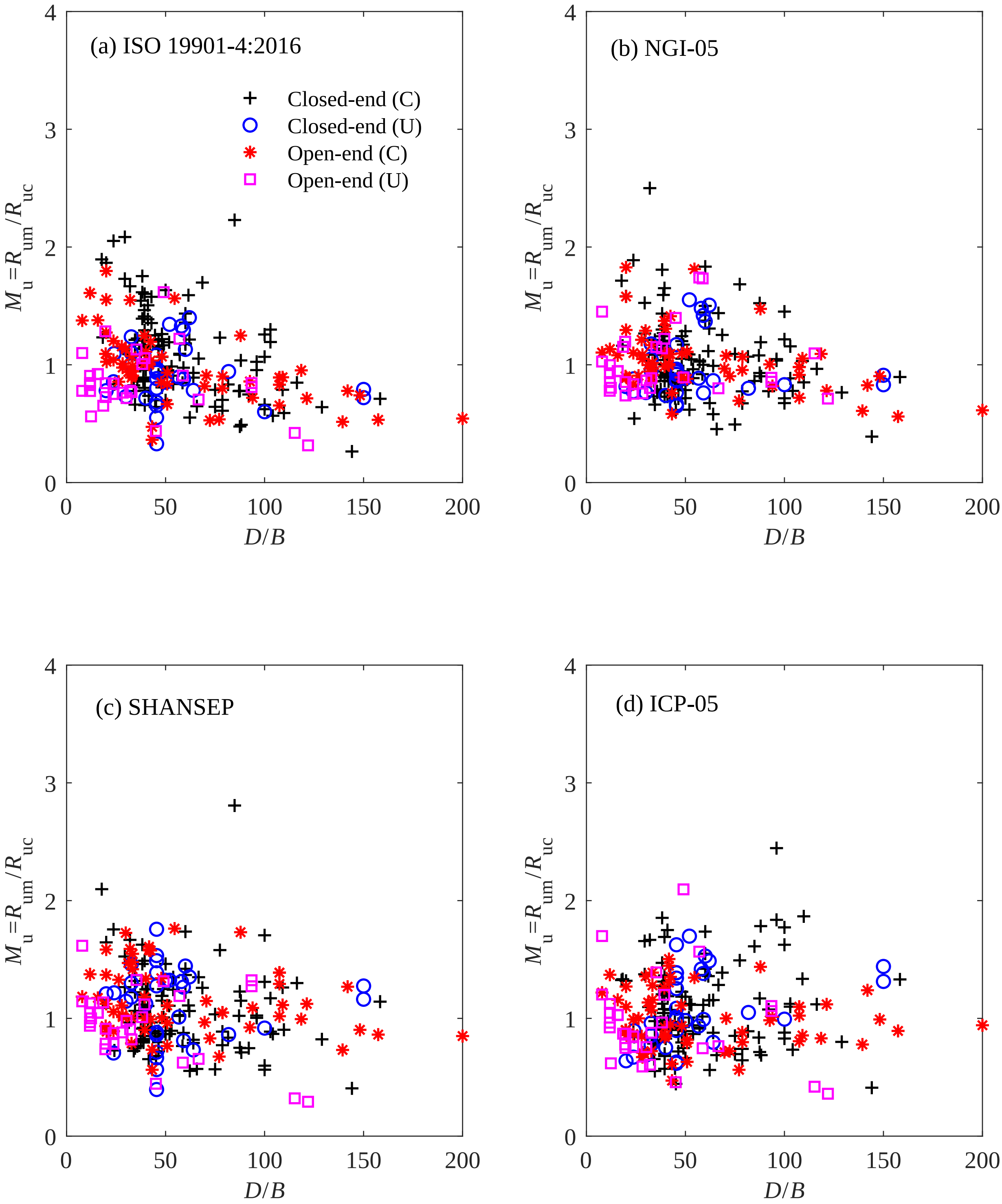

Fig. 4. Distributions of resistance model factor against pile slenderness ratio

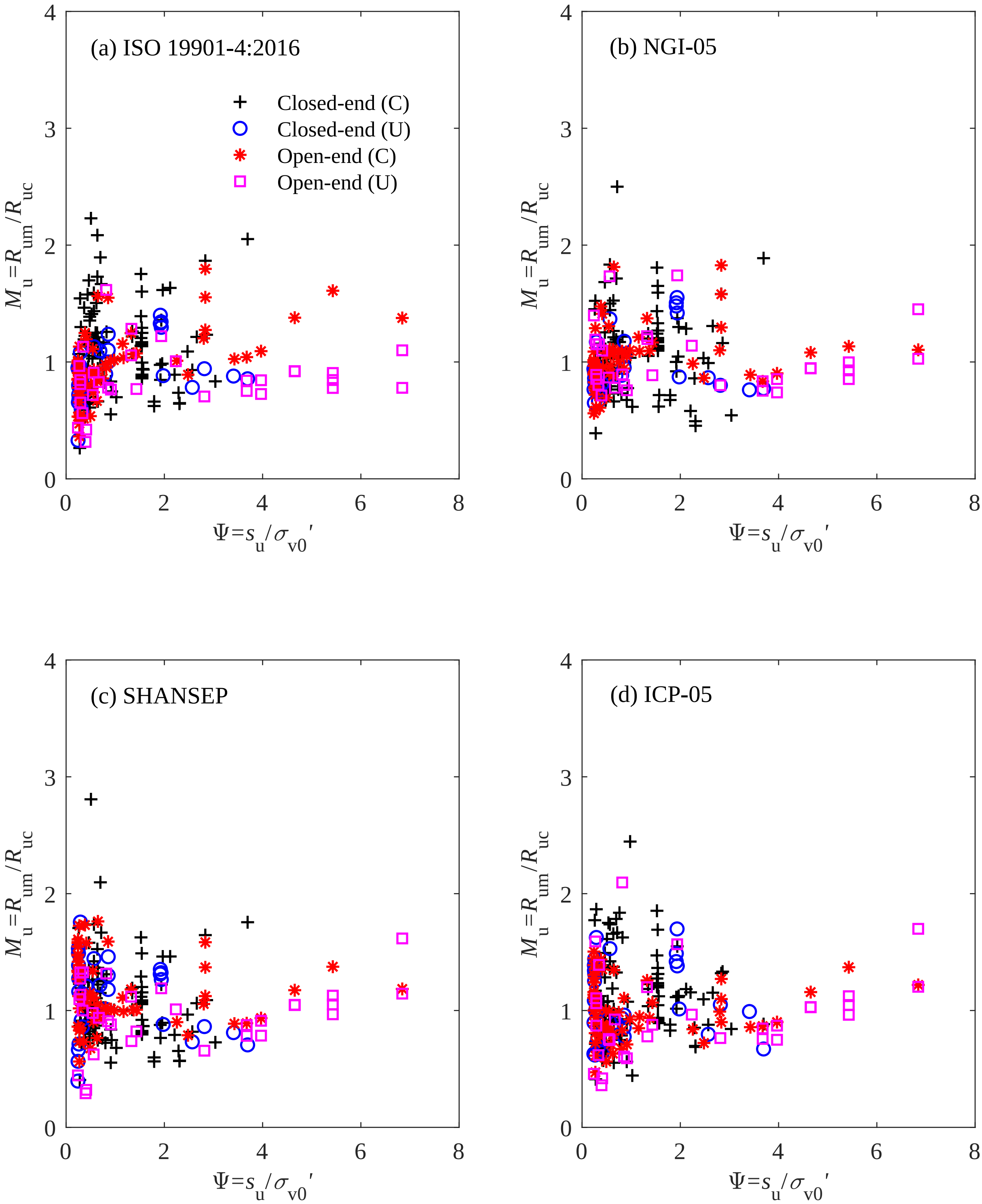

Fig. 5. Distributions of resistance model factor against undrained shear strength normalized by effective vertical stress

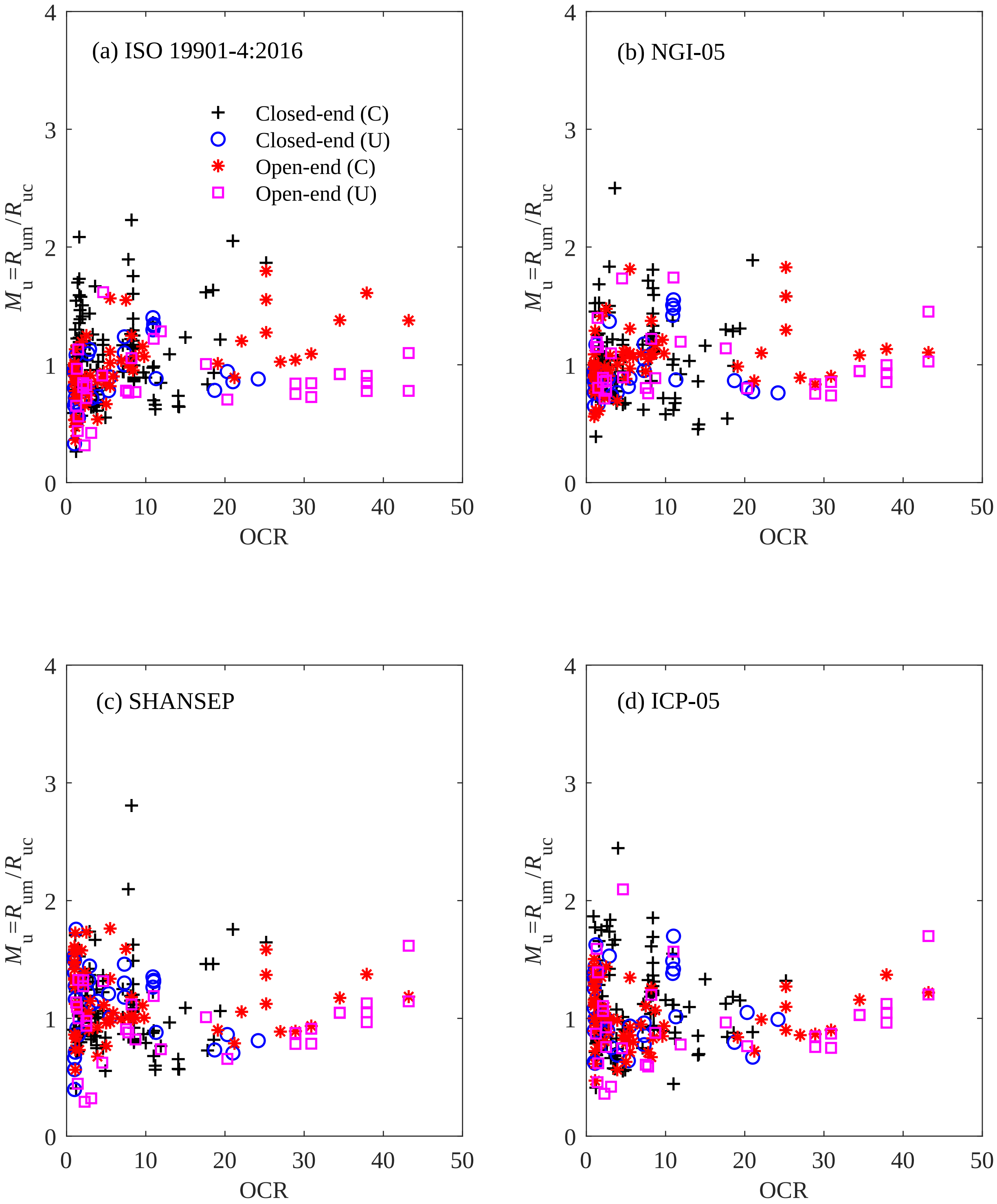

Fig. 6. Distributions of resistance model factor against overconsolidation ratio

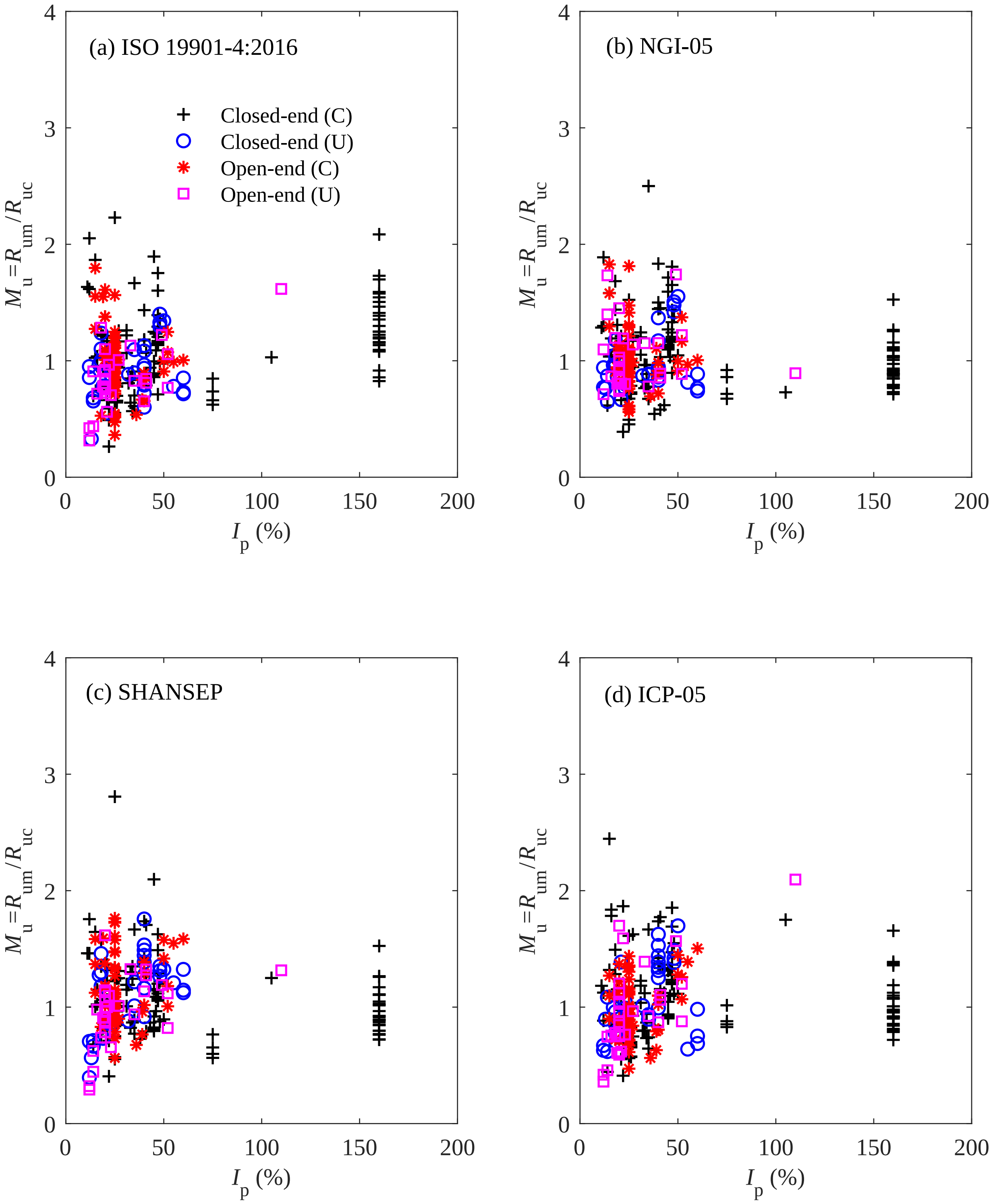

Fig. 7. Distributions of resistance model factor against plasticity index

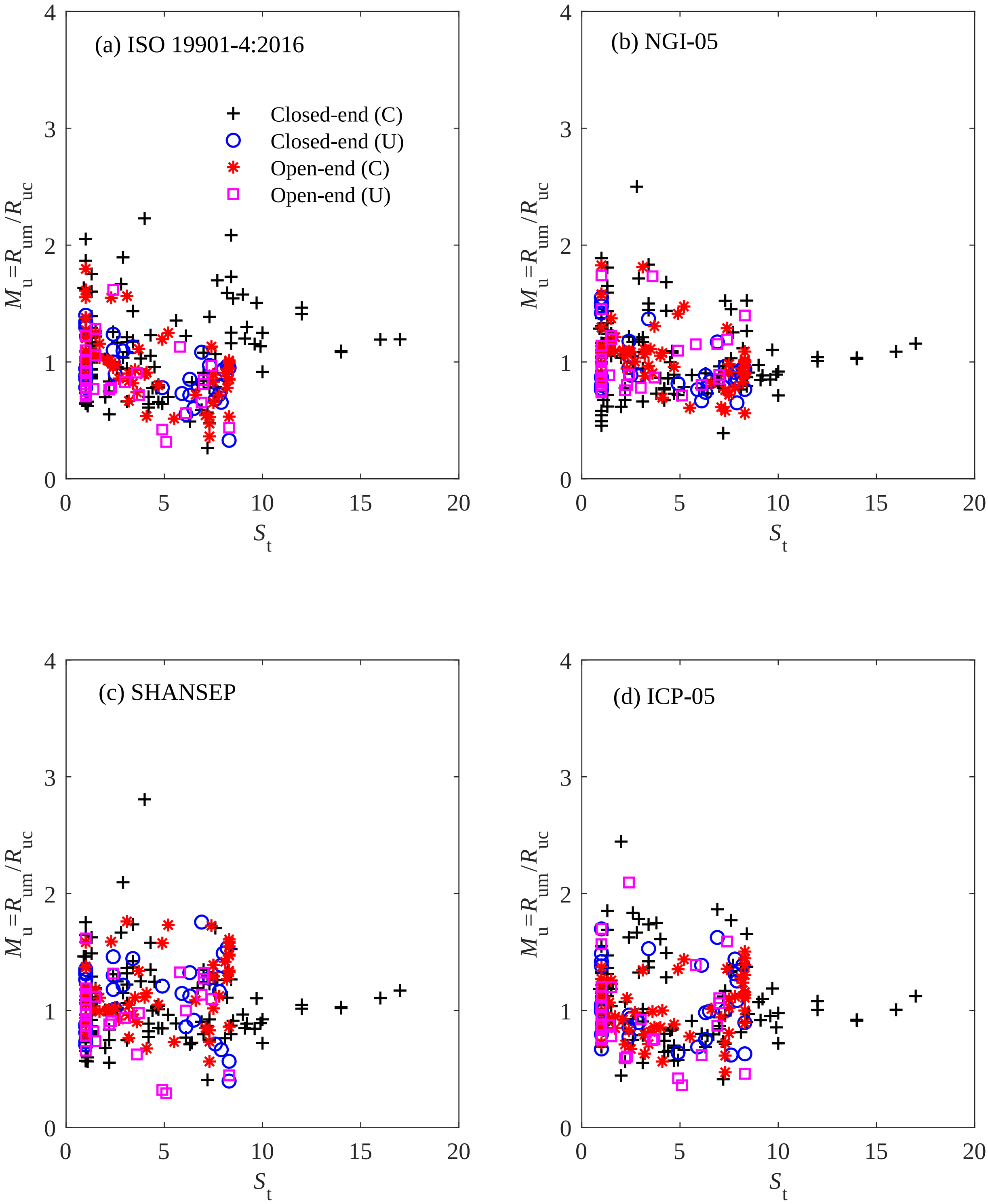

Fig. 8. Distributions of resistance model factor against sensitivity

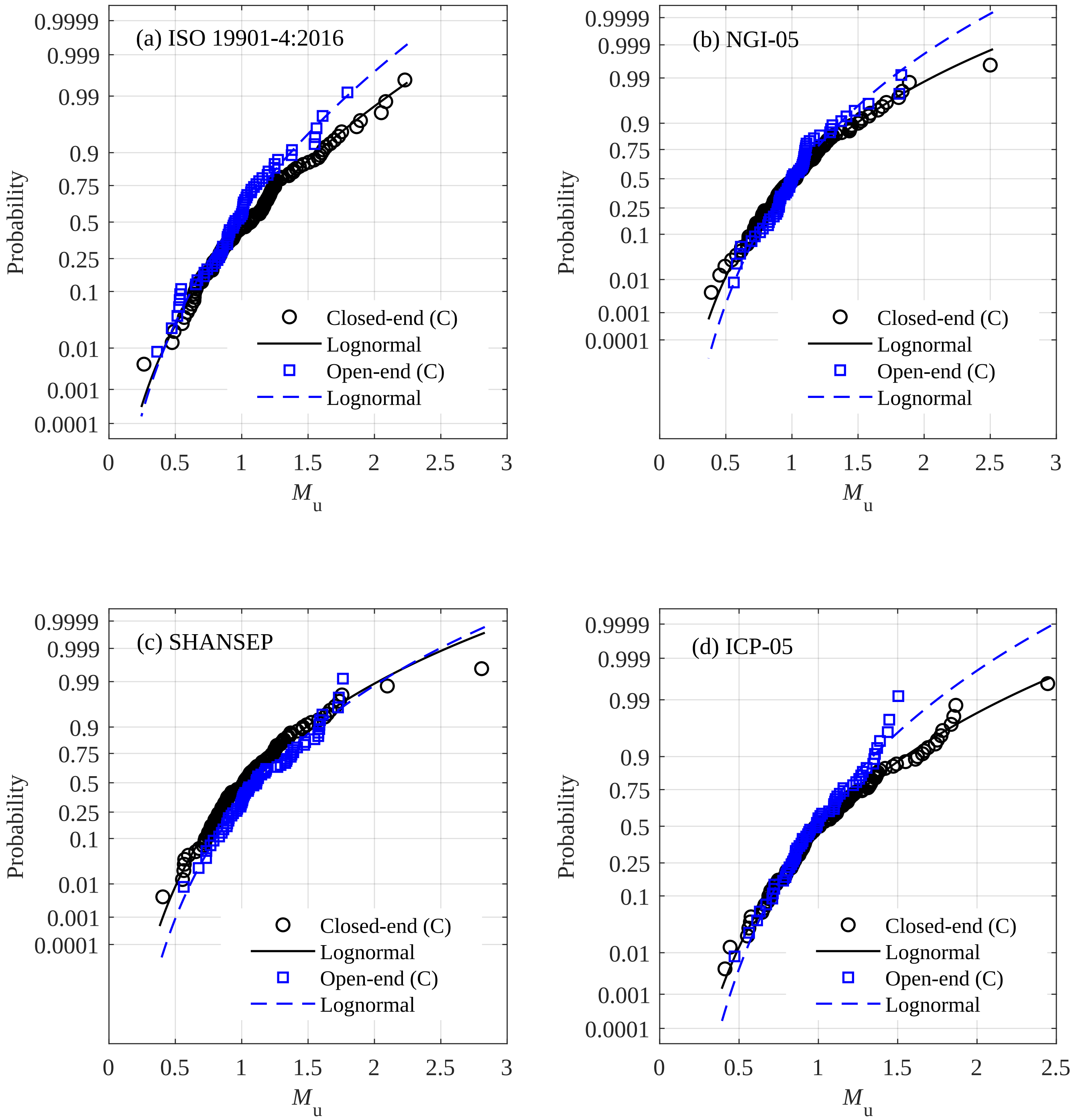

Fig. 9. Cumulative distributions of resistance model factor for driven piles in axial compression

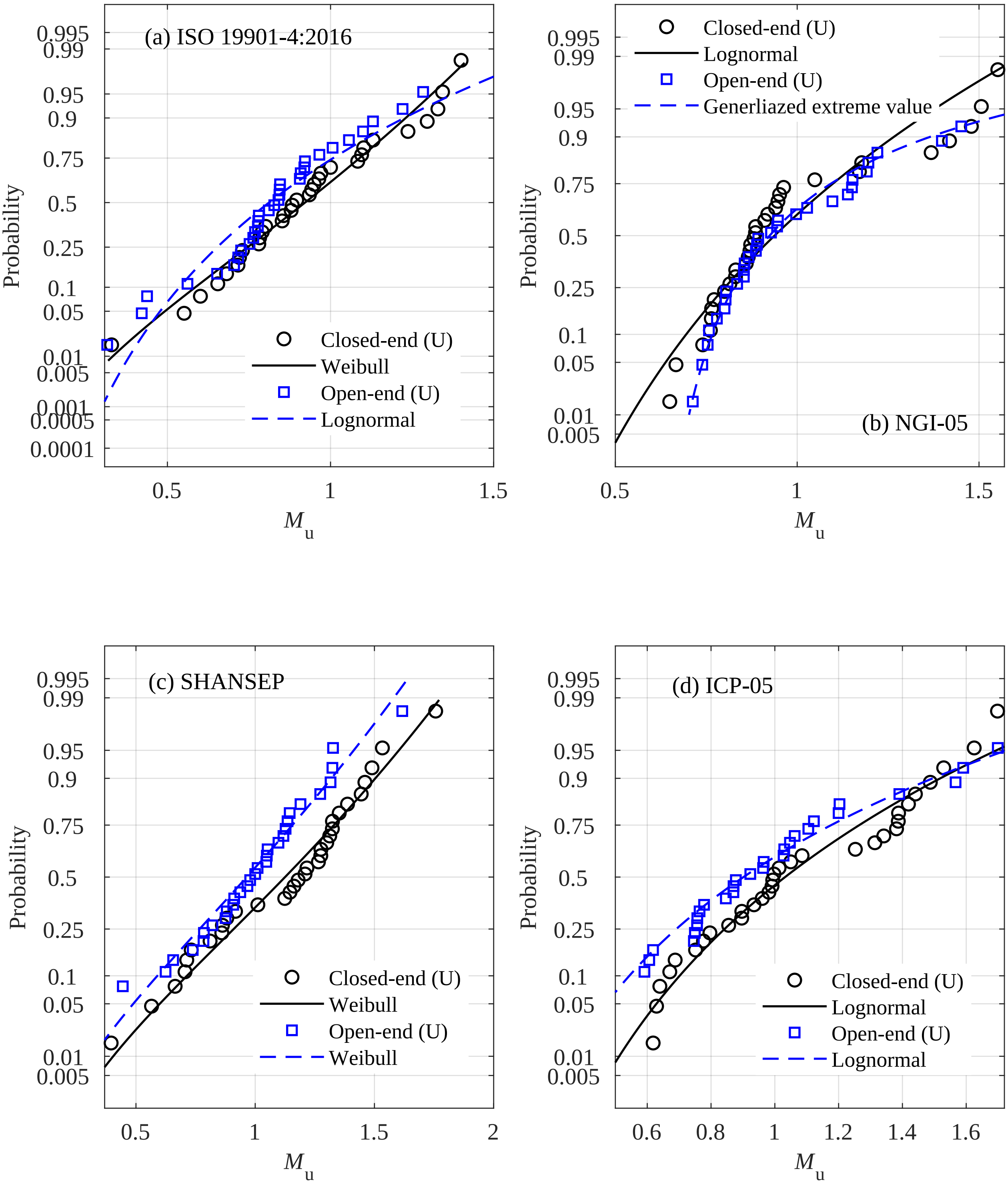

Fig. 10. Cumulative distributions of resistance model factor for driven piles in axial uplift

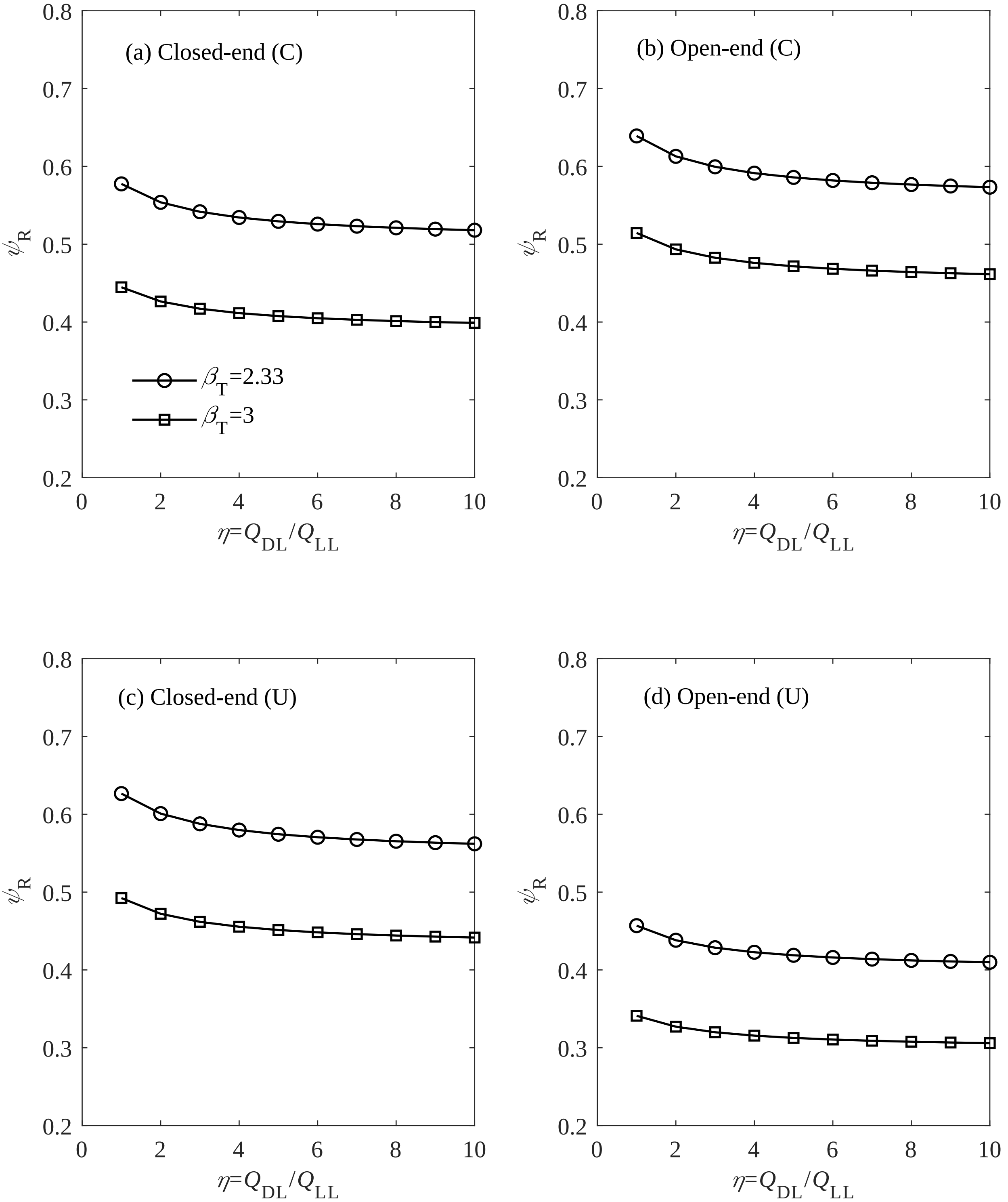

Fig. 11. Variation of resistance factor with dead to live load ratio

Table 1. Ranges of pile geometries and soil properties in the database

			Pile geometry		Soil parameters			
Load type	Pile tip	Number of load tests (N)	B (m)	D/B	I_p (%)	OCR	S_t	s_u/σ_{v0}'
Compression	Closed end	115	0.1–0.61	17.7–158.3	11–160	0.9–25.2	0.9–17	0.26-3.69
	Open end	60	0.11–0.81	7.9–200	15–60	1–43.2	1–8.3	0.24-6.84
Uplift	Closed end	32	0.1–0.4	20–150	12–60	1–24.2	1–8.3	0.24-3.69
	Open end	32	0.1–0.81	7.9–212.9	12–110	1.2–43.2	1–8.3	0.24-6.84

Note: B, pile diameter or width; D, embedment depth of pile; D/B, pile slenderness ratio; I_p, plasticity index; OCR, overconsolidation ratio; S_t, soil sensitivity; s_u, undrained shear strength; σ_{v0}', effective vertical stress.

Table 2. Statistics of resistance bias for static design methods of driven piles

Reference	Soil type	Pile tip	Material	Load type	N	Design method	Mean	COV
Paikowsky et al. (2004)	Clay	Closed/open end	Concrete	Compression	18	λ-Method	0.76	0.29
					17	α-API	0.81	0.26
					8	β-method	0.81	0.51
					18	α-Tomlinson	0.87	0.48
			Steel pipe	Compression	18	α-Tomlinson	0.64	0.5
					19	α-API	0.79	0.54
					12	β-method	0.45	0.6
					19	λ-method	0.67	0.55
					12	SPT-97	0.39	0.62
Dithinde et al. (2011)	Clay	Closed/open end	Concrete/steel	Compression	59	Static formula	1.17	0.26
Lehane et al. (2013)	Clay	Closed/open end	Concrete/steel	Compression/Uplift	75	API-00	1.13	0.46
						ICP-05	1.12	0.44
						CPT2000	1.04	0.39
						Almeida-96	1.08	0.37
						LCPC	2.22	0.45
						UWA-13	1.12	0.35
Karlsrud (2014)	Clay	Closed/open end	Steel pipe	Compression/Uplift	72	Proposed α-method	1.04	0.2
						Proposed β-method	1	0.22
Lehane et al. (2017)	Clay	Closed/open end	Concrete/steel	Compression/Uplift	23	API-00	1.54	0.33
					23	Fugro-96	1.21	0.24
					22	ICP-05	0.86	0.45
					47	NGI-05	1.17	0.33
					43	UWA-13	1.14	0.25
					43	Fugro-10	1.01	0.31
This work	Clay	Closed end	Concrete/steel pipe	Compression	115	ISO 19901-4:2016	1.08	0.34
					115	NGI-05	1.05	0.31
					115	SHANSEP	1.06	0.32
					115	ICP-05	1.08	0.33
				Uplift	32	ISO 19901-4:2016	0.92	0.27
					32	NGI-05	0.96	0.26
					32	SHANSEP	1.11	0.29

					32	ICP-05	1.08	0.29
		Open end	Steel pipe	Compression	60	ISO 19901-4:2016	0.97	0.3
This work	Clay	Open end	Steel pipe	Compression	60	NGI-05	1.03	0.25
					60	SHANSEP	1.16	0.25
					60	ICP-05	1	0.24
				Uplift	32	ISO 19901-4:2016	0.85	0.3
					32	NGI-05	1.01	0.27
					32	SHANSEP	0.96	0.3
					32	ICP-05	0.97	0.39
Paikowsky et al. (2004)	Clay	Open end	Steel-H	Compression	4	β-method	0.61	0.61
					16	λ-method	0.74	0.39
					17	α-Tomlinson	0.82	0.4
					16	α-API	0.9	0.41
					8	SPT-97	1.04	0.41
AbdelSalam et al. (2012)	Clay	Open end	Steel-H	Compression	20	α-API	1.15	0.52
Tang and Phoon (2018b)	Clay	Open end	Steel-H	Compression	26	α-API	1.1	0.4
Tang and Phoon (2018a)	Clay	Closed end	Steel square shaft (single-helix)	Compression	16	Torque-correlation	0.88	0.15
				Uplift	14	Torque-correlation	0.74	0.27
			Steel square shaft (multi-helix)	Compression	14	Torque-correlation	1.04	0.19
				Uplift	10	Torque-correlation	0.93	0.26
				Compression	49	Individual plate	1.25	0.41
		Open end	Steel pipe (single-helix)	Compression	75	Torque-correlation	1.09	0.26
				Uplift	54	Torque-correlation	0.92	0.23
			Steel pipe (multi-helix)	Compression	71	Torque-correlation	1.16	0.18
				Uplift	69	Torque-correlation	1.02	0.27
Paikowsky et al. (2004)	Sand	Closed/open end	Concrete	Compression	36	Nordlund	1.02	0.48
					35	β-method	1.1	0.44
					36	Meyerhof	0.61	0.61
					36	SPT-97	1.21	0.47
			Steel pipe	Compression	19	Nordlund	1.48	0.52
					20	β-method	1.18	0.62
					20	Meyerhof	0.94	0.59
					19	SPT-97	1.58	0.52
Dithinde et al. (2011)	Sand	Closed/open	Concrete/steel	Compression	28	Static formula	1.11	0.33

		end						
Lehane et al. (2017)	Sand	Closed/open end	Concrete/steel	Compression/Uplift	71	API-00	1.66	0.56
						Fugro-05	0.99	0.4
						ICP-05	1.04	0.27
Lehane et al. (2017)	Sand	Closed/open end	Concrete/steel	Compression/Uplift	71	NGI-05	0.99	0.34
						UWA-05	1.06	0.27
						Simplified ICP-05	1.2	0.31
						Offshore UWA-05	1.28	0.29
Tang and Phoon (2018c)	Sand	Open end	Concrete/steel pipe	Compression	16	ICP-05	1.07	0.24
					16	UWA-05	1.07	0.21
		Closed end	Concrete/steel pipe	Compression	52	ICP-05	1.1	0.31
					52	UWA-05	1	0.39
		Open end	Steel pipe	Uplift	19	ICP-05	1.36	0.38
					19	UWA-05	1.3	0.37
		Closed end	Steel pipe	Uplift	9	ICP-05	1.02	0.35
					9	UWA-05	1.02	0.37
Paikowsky et al. (2004)	Sand	Open end	Steel-H	Compression	19	Nordlund	0.94	0.4
					18	Meyerhof	0.81	0.38
					19	β-method	0.78	0.51
					18	SPT-97	1.35	0.43
AbdelSalam et al. (2012)	Sand	Open end	Steel-H	Compression	34	Nordlund	0.92	0.53
Tang and Phoon (2018b)	Sand	Open end	Steel-H	Compression	46	Nordlund	0.82	0.47
Tang and Phoon (2018a)	Sand	Closed end	Steel square shaft (single-helix)	Compression	6	Torque-correlation	1.51	0.39
				Uplift	7	Torque-correlation	1.2	0.56
			Steel square shaft (multi-helix)	Compression	10	Torque-correlation	1.54	0.39
				Uplift	10	Torque-correlation	1.06	0.22
				Compression	55	Individual plate	1.46	0.42
		Open end	Steel pipe (single-helix)	Compression	50	Torque-correlation	1.23	0.37
				Uplift	47	Torque-correlation	0.98	0.3
			Steel pipe (multi-helix)	Compression	49	Torque-correlation	1.51	0.26
				Uplift	51	Torque-correlation	1.2	0.24
Paikowsky et al. (2004)	Layered	Closed/open end	Concrete	Compression	33	α-Tomlinson/Nordlund	0.96	0.49
					80	α-API/Nordlund	0.87	0.48

					80	β-method/Thurman	0.81	0.38
					71	SPT-97	1.81	0.5
					30	FHWA CPT	0.84	0.31
		Closed/open end	Steel pipe	Compression	13	α-Tomlinson/Nordlund	0.74	0.59
					32	α-API/Nordlund	0.8	0.45
					29	β-method/Thurman	0.54	0.48
Paikowsky et al. (2004)	Layered	Closed/open end	Steel pipe	Compression	33	SPT-97	0.76	0.38
		Open end	Steel-H	Compression	20	α-Tomlinson/Nordlund	0.59	0.39
					34	α-API/Nordlund	0.79	0.44
					32	β-method/Thurman	0.48	0.48
					40	SPT-97	1.23	0.45
AbdelSalam et al. (2012)	Layered	Open end	Steel-H	Compression	26	API α/Nordlund	1.04	0.4
Tang and Phoon (2018b)	Layered	Open end	Steel-H	Compression	32	API α/Nordlund	0.92	0.4

Note: API, American Petroleum Institute; SPT, standard penetration test; α, ultimate shaft friction normalized to undrained shear strength; β, ultimate shaft friction normalized to vertical effective stress; λ, ultimate shaft friction normalized to the combination of undrained shear strength and vertical effective stress; CPT, cone penetration test; ICP, Imperia College Pile; UWA, University of Western Australia; NGI, Norwegian Geotechnical Institute; SHANSEP, stress history and normalized soil engineering parameter concept; LCPC, Laboratoire Central des Ponts et Chaussées.

Table 3. Resistance and efficiency factors in LRFD of driven piles in clay

Load type	Pile tip	Pile material/shape	N	Methods	M_u		β_T=2.33		β_T=3	
					Mean (μ)	COV	ψ_R	ψ_R/μ	ψ_R	ψ_R/μ
Compression	Closed end	Concrete/steel pipe	115	ISO 19901-4:2016	1.08	0.34	0.53	0.49	0.41	0.38
				NGI-05	1.05	0.31	0.55	0.52	0.43	0.41
				SHANSEP	1.06	0.32	0.54	0.51	0.42	0.4
				ICP-05	1.08	0.33	0.54	0.5	0.42	0.39
	Open end	Steel pipe	60	ISO 19901-4:2016	0.97	0.3	0.52	0.54	0.4	0.41
				NGI-05	1.03	0.25	0.61	0.59	0.49	0.48
				SHANSEP	1.16	0.25	0.68	0.59	0.55	0.47
				ICP-05	1	0.24	0.6	0.6	0.48	0.48
Uplift	Closed end	Concrete/steel pipe	32	ISO 19901-4:2016	0.92	0.27	0.52	0.57	0.41	0.45
				NGI-05	0.96	0.26	0.55	0.57	0.44	0.46
				SHANSEP	1.11	0.29	0.6	0.54	0.47	0.42
				ICP-05	1.08	0.29	0.59	0.55	0.46	0.43
	Open end	Steel pipe	32	ISO 19901-4:2016	0.85	0.3	0.45	0.53	0.35	0.41
				NGI-05	1.01	0.27	0.57	0.56	0.45	0.45
				SHANSEP	0.96	0.3	0.51	0.53	0.4	0.42
				ICP-05	0.97	0.39	0.43	0.44	0.32	0.33

Appendix A1

Table A1. Summary of compression load tests on driven piles in clay

		Pile information			Soil parameters						$^{\$}R_{uc}$ (kN)			
Reference	Site location	#Type	B (m)	D (m)	I_p (%)	σ_{v0}' (kN)	OCR	S_t	s_u (kPa)	R_{um} (kN)	(1)	(2)	(3)	(4)
Augustesen (2006)	Bangkok, Thailand	CE-Oc-C	0.58	14	38	53	17.8	1	161	1570	1882	2888	2158	1865
		CE-Sq-C	0.25	13	43	43	7.2	1.3	67	313	333	506	361	279
		CE-Sq-C	0.25	16	41	53	10	1	117	580	651	999	733	502
Saldivar and Jardine (2005)	Mexico city	CE-Sq-C	0.56	22	160	68	1.7	12	25	1274	870	1265	1255	1266
		CE-Sq-C	0.56	22	160	48	2	12	25	1048	743	1007	1000	971
		CE-Sq-C	0.56	23	160	46	2.1	10	29	993	795	1082	1074	1015
		CE-Sq-C	0.56	23	160	47	2	9.7	29	1231	818	1116	1114	1036
		CE-Sq-C	0.56	24	160	48	1.8	9	21	1104	700	1135	1143	1030
		CE-Sq-C	0.56	23	160	50	1.7	7.3	24	1040	750	1115	1126	1087
		CE-Sq-C	0.56	24	160	54	1.6	5.6	26	1162	858	1308	1307	1276
		CE-Sq-C	0.56	25	160	45	1.9	8.4	27	1048	838	1205	1204	1081
		CE-Sq-C	0.56	26	160	49	1.8	8.4	27	1049	904	1323	1315	1164
		CE-Sq-C	0.56	26	160	48	2	9.1	27	1058	881	1250	1246	1154
		CE-Sq-C	0.56	32	160	74	2.3	14	43	1858	1699	1795	1806	2018
		CE-Sq-C	0.56	32	160	74	2.3	14	43	1843	1699	1795	1806	2018
		CE-Sq-C	0.56	26	160	66	1.7	9.9	31	1255	1107	1407	1407	1466
		CE-Sq-C	0.34	10	160	55	1.6	8.4	35	540	259	354	354	326
		CE-Sq-C	0.34	10	160	55	1.6	8.4	35	448	259	354	354	326
		CE-Sq-C	0.56	26	160	69	1.5	10	31	1035	1130	1450	1436	1440
		CE-Sq-C	0.56	21	160	91	1.2	8.5	26	1433	928	1576	1570	1476
		CE-Sq-C	0.56	21	160	74	1.5	7	43	1207	1118	1525	1515	1435
		CE-Sq-C	0.56	20	160	87	1.3	8.1	64	1233	1438	1613	1616	1516
		CE-Sq-C	0.56	26	160	60	1.3	9.6	27	1135	984	1336	1344	1190
		CE-Sq-C	0.34	35	160	63	1.1	9.2	19	865	666	978	975	787
		CE-Sq-C	0.34	35	160	63	1.6	17	23	864	724	747	738	769
		CE-Sq-C	0.56	29	160	55	1.7	16	23	1151	966	1058	1040	1143
		CE-Sq-C	0.56	19	160	80	1.2	6.4	64	1093	1324	1495	1511	1390
		CE-Sq-C	0.56	20	160	65	1.3	6.1	25	943	771	1217	1227	1179
		CE-Sq-C	0.39	24	160	62	1.6	8.2	35	1163	731	1042	1048	856
Lehane et al. (2013)	Belgium	CE-Sq-C	0.35	6.4	46	50	15	1	143	625	507	538	574	469
		CE-Sq-C	0.35	11	46	70	13	1	173	1048	962	1015	1086	956
Lehane et al. (2013)	Shanghai, China	CE-Sq-C	0.25	23	18	82	3.8	2.2	76	558	746	719	747	519

Augustesen (2006)	Khulna	CE-Sq-C	0.25	22	16	72	2.6	2.9	50	560	540	470	487	314
		CE-Sq-C	0.25	24	16	88	3	2.6	67	720	754	687	703	392
		CE-Sq-C	0.25	24	15	90	4	2	88	900	878	869	896	368
		CE-Sq-C	0.36	27	18	108	1.5	4.6	47	900	1143	824	870	1057
		CE-Sq-C	0.31	27	18	108	1.5	4.6	47	760	979	704	744	908
		CE-Sq-C	0.31	24	18	97	1.6	4.3	45	1000	813	594	633	670
		CE-Sq-C	0.36	24	18	97	1.6	4.3	45	1000	950	695	741	779
	—	CE-C-C	0.26	14	34	87	2.4	7	25	255	281	265	189	271
		CE-C-C	0.26	14	34	87	2.4	7	25	235	281	265	189	271
		CE-C-C	0.47	23	27	59	7.1	2.6	45	863	917	913	856	1154
		CE-C-C	0.47	23	27	59	7.1	2.6	45	1069	917	913	856	1154
	Lillebælt, Denmark	CE-C-C	0.41	24	75	140	11.9	1	269	3237	3823	3518	4230	3188
		CE-C-C	0.41	17	75	111	14.1	1	254	1864	2532	2168	2852	2187
	Khorramshahr port, Iran	CE-C-C	0.38	13	26	74	3.9	4.4	33	335	431	390	335	512
		CE-C-C	0.38	15	26	81	3.6	4.7	35	335	510	460	394	586
		CE-C-C	0.38	19	26	98	3.1	5.2	38	515	737	656	535	777
		CE-C-C	0.38	15	26	81	3.6	4.7	35	400	512	463	396	588
		CE-C-C	0.38	17	26	88	3.4	4.9	36	380	592	531	449	660
		CE-C-C	0.38	15	26	81	3.6	4.7	35	410	510	460	394	586
	Maskinonge, Canada	CE-C-C	0.24	24	41	116	1.1	7.6	30	585	548	403	343	330
		CE-C-C	0.24	38	47	160	1.1	7.6	42	845	1188	943	740	635
	Nova Scotia, Canada	CE-C-C	0.24	12	11	85	18.5	0.9	180	1240	759	965	848	1048
		CE-C-C	0.34	13	12	92	17.6	1	181	1950	1207	1501	1334	1734
	Singapore	CE-C-C	0.33	28	25	87	8.2	4	44	2100	942	2435	748	1303
	Aalborg, Denmark	CE-C-C	0.38	31	25	165	4.9	2.2	150	2540	3050	2376	3038	2852
		CE-C-C	0.45	28	25	165	4.9	2.2	150	1800	3262	2668	3250	3204
	Egå Rensenanlæg, Denmark	CE-C-C	0.32	24	25	91	14.2	1	210	1400	2177	2839	2466	2009
		CE-C-C	0.38	25	25	84	14.1	1	194	1671	2579	3680	2929	2429
	Algade, Aalborg, Denmark	CE-C-C	0.26	13	25	86	9.7	1.3	135	660	706	921	762	740
	Drammen Stasjon, Norway	CE-C-C	0.34	49	22	295	1.2	7.2	82	1100	4171	2820	2711	2675
		CE-C-C	0.34	30	22	210	1.3	6.3	66	960	1958	1064	1350	1396
Saldivar and Jardine (2005)	Mexico city	CE-C-C	0.35	24	160	82	1.4	7.7	38	1316	775	1050	1045	948
Lehane et al. (2013)	Golden Ears Bridge	CE-C-C	0.36	36	27	124	3.3	2.4	102	3000	2386	2467	2290	1846
	Dublin, Ireland	CE-S-P	0.27	6.4	12	72	21	1	266	1350	658	715	769	1528
Lehane et al. (2013)	Sandpoint	CE-S-P	0.41	45	22	204	0.9	6.9	59	1915	3244	2251	2120	1026
	Sarapui	CE-S-P	0.11	4.5	105	11	1.9	3.8	5.9	7	6.8	9.6	5.6	4
Augustesen (2006)	—	CE-S-P	0.27	13	32	79	2.6	6.7	24	206	255	249	173	259

		CE-S-P	0.31	14	14	138	11	2	141	697	998	1131	1025	1571
		CE-S-P	0.31	5.5	45	43	7.8	2.9	30	216	114	126	103	163
	Lillebælt, Denmark	CE-S-P	0.27	27	75	154	11.2	1.1	276	1776	2851	2633	3148	2143
		CE-S-P	0.27	27	75	154	11.2	1.1	276	1884	2851	2633	3148	2143
	Houston, USA	CE-S-P	0.27	13	31	81	8.1	1.5	109	670	628	637	665	646
		CE-S-P	0.27	13	31	81	8.1	1.5	109	765	628	637	665	646
		CE-S-P	0.27	13	31	81	8.1	1.5	109	792	628	637	665	646
	Cowden, UK	CE-S-P	0.46	9.2	15	48	25.2	1	136	1670	895	1056	1015	1266
	Khorramshahr port, Iran	CE-S-P	0.35	14	26	76	3.8	4.5	34	400	418	401	321	483
	Maskinonge, Canada	CE-S-P	0.22	24	41	116	1.1	7.6	30	390	495	378	309	292
	St Alban, Canada	CE-S-P	0.22	7.6	21	31	4.6	3.1	20	47	71	71	63	85
		CE-S-P	0.22	7.6	21	31	4.6	3.1	20	67	71	71	63	85
		CE-S-P	0.22	7.6	21	31	4.6	3.1	20	77	71	71	63	85
		CE-S-P	0.22	7.6	21	31	4.6	3.1	20	83	71	71	63	85
		CE-S-P	0.22	7.6	21	31	4.6	3.1	20	86	71	71	63	85
	Cowden, UK	CE-S-P	0.1	6.2	19	50	19.4	1	133	136	112	104	128	118
		CE-S-P	0.1	6.4	19	51	18.6	1	131	108	116	109	132	123
	Lower arrow lake, Canada	CE-S-P	0.61	48	35	156	3.8	4.2	75	3160	5183	4697	4093	4907
		CE-S-P	0.61	48	35	156	3.8	4.2	75	3649	5200	4712	4111	4926
	Canons park, UK	CE-S-P	0.1	5.3	50	45	11	1	88	68	69	65	76	61
		CE-S-P	0.1	6	48	48	10.9	1	93	110	81	80	90	71
		CE-S-P	0.1	5.9	48	48	10.9	1	92	78	80	78	89	70
		CE-S-P	0.17	6.5	47	63	8.4	1.3	96	189	166	161	179	157
		CE-S-P	0.17	6.5	47	63	8.4	1.3	96	200	166	161	179	157
		CE-S-P	0.17	6.5	47	63	8.4	1.3	96	231	166	161	179	157
		CE-S-P	0.17	6.5	47	63	8.4	1.3	96	291	166	161	179	157
		CE-S-P	0.17	6.7	47	63	8.4	1.3	97	194	171	166	184	162
		CE-S-P	0.17	6.7	47	63	8.4	1.3	97	197	171	166	184	162
		CE-S-P	0.17	6.7	47	63	8.4	1.3	97	200	171	166	184	162
		CE-S-P	0.17	6.7	47	63	8.4	1.3	97	221	171	166	184	162
		CE-S-P	0.17	6.7	47	63	8.4	1.3	97	274	171	166	184	162
		CE-S-P	0.17	6.6	45	68	8.5	1.3	105	159	185	145	200	176
		CE-S-P	0.17	6.6	45	68	8.5	1.3	105	161	185	145	200	176
Augustesen (2006)	Canons park, UK	CE-S-P	0.17	6.6	45	68	8.5	1.3	105	163	185	145	200	176
		CE-S-P	0.17	6.6	45	68	8.5	1.3	105	165	185	145	200	176
		CE-S-P	0.17	6.6	45	68	8.5	1.3	105	184	185	145	200	176
		CE-S-P	0.17	6.6	45	68	8.5	1.3	105	231	185	145	200	176
	Napoli, Italy	CE-S-P	0.38	49	33	179	3.1	4.2	85	2348	3668	3071	2856	2934

	Livorno, Italy	CE-S-P	0.48	50	34	208	1.9	7.2	58	2400	4231	3084	2765	3269
		CE-S-P	0.49	57	33	213	1.9	7.2	59	4200	4952	4351	3231	3752
	Bothkennar, UK	CE-S-P	0.1	6	40	30	2.9	3.4	17	27	23	18	19	19
		CE-S-P	0.1	6	40	30	2.9	3.4	17	33	23	18	19	19
		CE-S-P	0.1	3.2	35	21	3.6	2.8	15	15	9	6	9	9
		CE-S-P	0.1	6	40	30	2.9	3.4	17	26	22	18	19	19
	Motorvegbru, Drammen, Norway	CE-S-P	0.4	35	25	240	1.1	7.3	65	1350	2837	1451	1800	1890
		CE-S-P	0.4	35	25	240	1.1	7.3	65	2210	2837	1451	1800	1890
	—	OE-S-P	0.76	20	25	144	1	8.3	35	1567	1831	1727	1180	1567
		OE-S-P	0.46	22	25	148	1	8.3	35	976	1150	1093	728	880
		OE-S-P	0.61	19	25	142	1	8.3	34	1269	1352	1272	863	1118
		OE-S-P	0.36	15	25	448	1	8.3	109	1965	1941	1805	1222	1507
		OE-S-P	0.36	12	25	718	1	8.3	172	2368	2506	2330	1602	2045
		OE-S-P	0.31	44	25	162	1.1	8.2	40	1313	1687	1590	1035	1060
		OE-S-P	0.61	96	25	355	1	8.3	86	8516	15991	15190	9878	9533
		OE-S-P	0.61	74	25	273	1.1	7.8	70	7080	9905	9074	6303	6326
		OE-S-P	0.77	23	25	651	1.1	7.4	176	11276	9965	8748	6535	8311
		OE-S-P	0.33	66	25	222	1.2	7.1	63	2205	4056	3595	2595	2342
		OE-S-P	0.33	31	25	154	1.4	6.6	46	971	1350	1185	892	959
		OE-S-P	0.33	46	25	149	1.6	5.5	54	1097	2128	1803	1499	1410
		OE-S-P	0.33	29	25	104	2.5	5.2	40	1252	1003	849	723	871
		OE-S-P	0.33	14	25	112	1.9	4.9	46	637	533	451	404	471
		OE-S-P	0.33	18	25	51	5.5	3.1	33	638	408	352	362	474
		OE-S-P	0.61	48	25	152	2.8	4.7	65	3802	4756	3978	3621	4317
		OE-S-P	0.11	12	25	44	4.7	4	22	59	66	56	53	69
		OE-S-P	0.17	12	25	33	3	4.1	16	70	77	65	61	70
		OE-S-P	0.35	14	25	59	5.5	3.7	32	401	361	307	300	468
		OE-S-P	0.27	40	25	297	2.8	3.6	165	2868	3874	3173	3177	2895
		OE-S-P	0.61	31	25	92	4.7	3.5	52	2022	2166	1821	1821	2472
		OE-S-P	0.33	23	25	91	5.5	3.4	53	691	845	714	715	969
		OE-S-P	0.33	26	25	98	5.9	3.2	62	971	1078	910	927	1217
		OE-S-P	0.27	25	25	244	3.9	2.7	182	2048	2386	2041	2219	2082
Augustesen (2006)	—	OE-S-P	0.53	15	25	66	8.2	2.5	53	819	839	755	798	1221
		OE-S-P	0.27	32	25	141	8.4	2.4	115	1728	1814	1582	1739	2081
		OE-S-P	0.33	13	25	110	5.5	2.1	107	798	786	726	798	864
		OE-S-P	0.61	17	25	86	9.6	1.7	99	2085	1804	1720	1879	2458
		OE-S-P	0.33	14	25	112	6.9	1.7	131	1015	980	930	1024	1071
		OE-S-P	0.27	13	25	80	9.8	1.4	110	674	630	615	671	721
		OE-S-P	0.61	20	25	104	21.2	1	258	4187	4699	4852	5314	5799

		OE-S-P	0.45	9.1	25	54	27	1	185	1166	1137	1310	1314	1360
		OE-S-P	0.76	18	25	116	22.1	1	325	8212	6832	7467	7779	8288
	Empire, LA, USA	OE-S-P	0.36	15	60	256	1	8.3	62	1113	1107	1107	702	740
		OE-S-P	0.36	15	50	448	1	8.3	108	1936	1935	1945	1227	1338
		OE-S-P	0.36	12	55	616	1	8.3	148	2127	2150	2201	1374	1532
		OE-S-P	0.36	12	50	719	1	8.1	178	2354	2594	2574	1661	1839
	Cowden, UK	OE-S-P	0.46	9.2	15	48	25.2	1	136	1140	895	880	1015	1266
		OE-S-P	0.46	9.2	15	48	25.2	1	136	1390	895	880	1015	1266
		OE-S-P	0.46	9.2	15	48	25.2	1	136	1608	895	880	1015	1266
	Izmir, Turkey	OE-S-P	0.53	17	19	62	7.5	2.3	53	1410	910	1494	887	1276
		OE-S-P	0.53	15	20	57	7.8	2.2	52	780	773	744	771	1099
	Sumatra, Indonesia	OE-S-P	0.4	43	40	131	2.3	7.5	35	1225	1872	1702	1203	1520
		OE-S-P	0.4	43	40	131	2.3	7.5	35	1555	1872	1702	1203	1520
		OE-S-P	0.4	43	40	131	2.3	7.5	35	1670	1872	1702	1203	1520
		OE-S-P	0.4	43	40	131	2.3	7.5	35	1670	1872	1702	1203	1520
	Lower arrow lake, Canada	OE-S-P	0.61	31	39	94	5	3.2	59	1558	2339	1769	2036	2470
		OE-S-P	0.61	31	39	94	5	3.2	59	1958	2339	1769	2036	2470
		OE-S-P	0.61	47	36	150	3.9	4.1	74	2626	4895	3781	3888	4662
	West Sole, North sea, UK	OE-S-P	0.76	6	20	38	43.2	1	260	3051	2217	2764	2576	2503
		OE-S-P	0.76	9	20	56	37.9	1	304	5471	3399	4827	3980	3992
		OE-S-P	0.76	12	20	75	34.5	1	349	6681	4846	6182	5692	5771
		OE-S-P	0.76	15	20	93	30.9	1	369	6788	6213	7523	7261	7535
		OE-S-P	0.76	18	20	111	28.9	1	408	8344	8012	10010	9365	9631
	Pentre, UK	OE-S-P	0.76	55	18	320	1.1	7.3	87	6030	11418	6678	7266	8352
	Tilbrook, UK	OE-S-P	0.76	30	27	212	19.1	1	478	16131	15969	16374	17915	19205
	Kontich, Belgium	OE-S-P	0.61	24	52	124	8.2	1.5	164	4840	3881	3525	4098	3849
		OE-S-P	0.61	20	52	109	8.7	1.4	156	3380	3149	2897	3357	3166
	Drammen, Norway	OE-S-P	0.81	35	25	240	1.1	7.3	65	2150	5922	3689	3815	4561
		OE-S-P	0.81	35	25	240	1.1	7.3	65	2800	5922	3689	3815	4561

Note: In Tables A1-A2, OE-S-P=open-end steel pipe pile, CE-S-P=closed-end steel pipe pile, CE-Oc-C=closed-end octagonal concrete pile, CE-Sq-C=closed-end square concrete pile, and CE-C-C=closed-end circular concrete pile. (1)=ISO 19901-4:2016, (2)=NGI-05 (Karlsrud et al. 2005), (3)=the SHANSEP-based approach (Saye et al. 2013), and (4)=ICP-05 (Jardine et al. 2005).

Table A2. Summary of uplift load tests on driven piles in clay

		Pile information			Soil parameters						\$ R_{uc} (kN)			
Reference	Site location	[#]Type	B (m)	D (m)	I_p (%)	σ_{v0}' (kN)	OCR	S_t	s_u (kPa)	R_{um} (kN)	(1)	(2)	(3)	(4)
Augustesen (2006)	Montreal, Canada	CE-C-C	0.3	17	35	67	5.5	2.5	54	458	511	517	453	490
	Göteborg, Sweden	CE-C-C	0.34	34	40	146	1.3	6.5	45	900	1497	1083	981	906

	Bangkok, Thailand	CE-C-C	0.4	8	55	39	5.3	4.9	16	110	141	135	91	172
		CE-C-C	0.4	12	60	48	3.9	5.9	16	165	226	216	144	240
		CE-C-C	0.4	16	60	57	3.2	6.3	18	245	342	331	218	326
		CE-C-C	0.4	20	60	67	2.8	6.3	21	425	499	480	321	433
	Belfast, Ireland	CE-Sq-C	0.25	6	35	32	2.7	2.9	22	69	63	78.3	56.7	77
	Pentre A5, UK	CE-S-P	0.22	10	14	198	1.1	7.6	52	154	226	177	216	249
	Pentre A6, UK	CE-S-P	0.22	10	17	251	1.1	7.3	69	361	372	375	283	362
	Tilbrook, UK	CE-S-P	0.22	13	23	118	24.2	1	402	1238	1408	1626	1527	1249
	Tilbrook, UK	CE-S-P	0.22	18	23	151	20.3	1	425	1995	2117	2493	2313	1900
	Tilbrook B, UK	CE-S-P	0.22	10	32	298	11.3	1	589	1684	1908	1931	1912	1662
	Onsøy, Norway	CE-S-P	0.22	10	40	62	1.2	6.9	18	130	120	111	74	80
		CE-S-P	0.22	33	40	113	1.1	7.8	29	465	645	560	400	354
		CE-S-P	0.22	33	40	113	1.1	7.8	29	510	645	560	400	354
		CE-S-P	0.22	10	40	100	1	8.2	25	161	167	170	105	116
		CE-S-P	0.22	10	40	139	1	8	35	216	231	235	145	161
		CE-S-P	0.22	10	40	177	1	7.9	45	258	322	300	186	206
	Lierstranda, Norway	CE-S-P	0.22	10	21	75	1.5	6.1	25	86	156	129	100	62
		CE-S-P	0.22	10	14	128	1	7.9	32	89	136	137	134	82
		CE-S-P	0.22	10	13	181	1	8.3	44	104	316	136	184	116
		CE-S-P	0.22	10	12	237	1	8.3	57	95	100	101	240	151
	Haga, Norway	CE-S-P	0.15	4.9	18	49	7.3	2.4	42	59	59	62	50	76
		CE-S-P	0.15	4.9	18	49	7.3	2.4	42	65	59	62	50	76
		CE-S-P	0.15	4.9	18	49	7.3	2.4	42	73	59	62	50	76
	Cowden, UK	CE-S-P	0.1	6.4	19	51	18.7	1	131	90	115	104	123	113
	Canons park, UK	CE-S-P	0.1	5.2	50	45	11	1	87	90	67	58	68	53
		CE-S-P	0.1	6.2	48	49	10.9	1	94	119	85	79	88	80
		CE-S-P	0.1	5.9	48	48	10.9	1	93	105	81	74	83	76
Augustesen (2006)	Canons park, UK	CE-S-P	0.1	5.8	48	48	11	1	92	105	79	71	80	74
	Bothkennar, UK	CE-S-P	0.1	6	40	30	2.9	3.4	17	26	23	19	18	17
Lehane et al. (2013)	Dublin, Ireland	CE-S-P	0.27	6.4	12	72	21	1	266	446	521	578	632	665
Augustesen (2006)	Tilbrook, UK	OE-S-P	0.27	18	23	151	20.3	1	425	1891	2684	2363	2883	2475
	Onsøy, Norway	OE-S-P	0.81	15	40	62	1.2	6.9	18	469	719	407	413	539
	Lierstranda, Norway	OE-S-P	0.81	10	21	75	1.5	6.1	25	374	666	465	374	605
	Izmir, Turkey	OE-S-P	0.53	17	19	62	7.5	2.3	53	710	910	884	782	1171
		OE-S-P	0.53	15	20	57	7.8	2.2	52	590	773	779	670	998
	West Sole, UK	OE-S-P	0.76	6	20	38	43.2	1	260	2438	2217	1680	1508	1435
		OE-S-P	0.76	9	20	56	37.9	1	304	2873	3399	3096	2731	2743
		OE-S-P	0.76	12	20	75	34.5	1	349	4466	4846	4727	4259	4338
		OE-S-P	0.76	15	20	93	30.9	1	369	5240	6213	6140	5746	6019

		OE-S-P	0.76	18	20	111	28.9	1	408	6734	8012	8065	7691	7957
		OE-S-P	0.76	6	20	38	43.2	1	260	1726	2217	1680	1508	1435
		OE-S-P	0.76	9	20	56	37.9	1	304	2642	3399	3096	2731	2743
		OE-S-P	0.76	9	20	56	37.9	1	304	3079	3399	3088	2731	2743
		OE-S-P	0.76	12	20	75	34.5	1	349	4457	4846	4706	4259	4338
		OE-S-P	0.76	15	20	93	30.9	1	369	4510	6213	6102	5746	6019
		OE-S-P	0.76	18	20	111	28.9	1	408	6023	8012	7989	7691	7957
	Tilbrook, UK	OE-S-P	0.76	29	27	219	17.6	1	489	16200	16098	14220	16039	16788
	Canons park, UK	OE-S-P	0.1	5.7	49	47	11	1	91	94	77	54	79	60
	Kontich, Belgium	OE-S-P	0.61	24	52	124	8.2	1.5	164	4100	3881	3359	3666	3417
		OE-S-P	0.61	20	52	109	8.7	1.4	156	2420	3149	2730	2948	2757
	Long beach, USA	OE-S-P	0.76	23	16	673	2.5	3.7	365	10710	14934	12361	10941	14164
	West Delta, USA	OE-S-P	0.76	71	41	128	2.1	7	37	5030	5958	5655	3800	4552
		OE-S-P	0.76	71	41	128	2.1	7	37	4850	5982	5669	3811	4566
	Belfast, Ireland	OE-S-P	0.17	2.0	35	33	2.5	3	22	12	14.5	15.4	12.8	13
Karlsrud (2012)	Børsa, Norway	OE-S-P	0.41	50	12	230	2.28	5.1	91	1448	4588	2031	4962	4022
	Vigda, Norway	OE-S-P	0.46	27	14	112	4.51	3.6	62.8	1461	1608	843	2341	1958
		OE-S-P	0.46	53	12	212	3.11	4.9	86.9	2172	5154	1980	6769	5176
	Onsøy 2, Norway	OE-S-P	0.51	18	33	68	1.47	5.8	23.5	634	561	551	478	456
	Stjørdal, UK	OE-S-P	0.51	23	14	136	1.41	8.3	32.7	527	1204	377	1185	1151
	Cowden, UK	OE-S-P	0.46	9	18	85	11.9	1.5	113	873	680	730	1183	1122
	Femern, Germany	OE-S-P	0.51	25	110	104	4.62	2.4	85	3028	1873	3391	2301	1445
	Oromieh, Iran	OE-S-P	0.31	66	22	178	1.3	7.4	48	2825	2925	2371	2574	1776

Appendix A2

Table A3. Correlation between M_u and input parameters for driven piles in clay

				B		D/B		I_p		OCR		S_t		s_u/σ_{v0}'	
Load type	Pile tip	N	Design method	r	p	r	p	r	p	r	p	r	p	r	p
Compression	Closed-end	115	ISO 19901-4:2016	-0.1	0.27	**-0.41**	**0**	**0.34**	**0**	0.04	0.65	0.04	0.64	0.18	0.05
			NGI-05	**-0.46**	**0**	**-0.22**	**0.02**	-0.06	0.51	0.13	0.17	-0.18	0.06	**0.19**	**0.04**
			SHANSEP	**-0.35**	**0**	-0.14	0.14	-0.13	0.16	-0.04	0.7	0.03	0.73	-0.1	0.28
			ICP-05	**-0.44**	**0**	0.03	0.72	0.12	0.19	0.01	0.94	-0.12	0.19	0.16	0.08
	Open-end	60	ISO 19901-4:2016	0.06	0.64	**-0.71**	**0**	**-0.34**	**0.01**	**0.59**	**0**	**-0.57**	**0**	**0.58**	**0**
			NGI-05	-0.11	0.4	**-0.42**	**0**	-0.16	0.22	**0.42**	**0**	**-0.41**	**0**	**0.41**	**0**
			SHANSEP	-0.17	0.2	-0.23	0.07	0.04	0.73	-0.23	0.08	**0.29**	**0.02**	**-0.28**	**0.03**
			ICP-05	-0.16	0.21	-0.19	0.15	0.09	0.47	-0.23	0.07	0.25	0.06	-0.23	0.08
Uplift	Closed-end	32	ISO 19901-4:2016	**-0.61**	**0**	0.03	0.88	0.15	0.41	**0.38**	**0.03**	**-0.48**	**0.01**	**0.42**	**0.02**
			NGI-05	**-0.65**	**0**	0.16	0.37	0.19	0.31	0.12	0.5	-0.23	0.2	0.15	0.41
			SHANSEP	-0.27	0.14	0.01	0.95	**0.55**	**0**	-0.1	0.59	0.01	0.94	-0.06	0.74
			ICP-05	**-0.48**	**0.01**	**0.55**	**0**	**0.37**	**0.04**	-0.07	0.71	-0.04	0.84	-0.02	0.91
	Open-end	32	ISO 19901-4:2016	-0.15	0.41	-0.06	0.73	**0.37**	**0.04**	0.25	0.17	-0.25	0.16	0.25	0.17
			NGI-05	-0.15	0.42	0.09	0.64	0.08	0.68	-0.07	0.72	0.11	0.53	-0.07	0.69
			SHANSEP	0.33	0.07	-0.2	0.28	**0.62**	**0**	0.04	0.83	0.01	0.96	0.07	0.69
			ICP-05	0.07	0.69	-0.14	0.43	**0.64**	**0**	0.24	0.19	-0.2	0.26	0.26	0.15

Note: Bold values indicate potential correlation between the model factor and the underlying parameters.